

Impact of (magneto-)thermoelectric effect on diffusion of conserved charges in hot and dense hadronic matter

He-Xia Zhang,^{1,2,*} Ke-Ming Shen,^{3,†} Yu-Xin Xiao,^{4,‡} and Ben-Wei Zhang^{4,§}

¹*Key Laboratory of Atomic and Subatomic Structure and Quantum Control (MOE), Guangdong Basic Research Center of Excellence for Structure and Fundamental Interactions of Matter, Institute of Quantum Matter, South China Normal University, Guangzhou 510006, China*

²*Guangdong-Hong Kong Joint Laboratory of Quantum Matter, Guangdong Provincial Key Laboratory of Nuclear Science, Southern Nuclear Science Computing Center, South China Normal University, Guangzhou 510006, China*

³*School of Science, East China University of Technology, Nanchang 330013, China*

⁴*Key Laboratory of Quark & Lepton Physics (MOE) and Institute of Particle Physics, Central China Normal University, Wuhan 430079, China*

We investigate the thermoelectric effect, which describes the generation of an electric field induced by temperature and conserved charge chemical potential gradients, in the hot and dense hadronic matter created in heavy-ion collisions. Utilizing the Boltzmann kinetic theory within the repulsive mean-field hadron resonance gas model, we evaluate both the diffusion thermopower matrix and diffusion coefficient matrix for the baryon number (B), electric charge (Q), and strangeness (S). The Landau-Lifshitz choice for the rest frame of the fluid is enforced in the derivation. We find that the thermoelectric effect hinders the diffusion processes of multiple conserved charges, particularly reducing the coupling between electric charge and baryon number (strangeness) in baryon (strangeness) diffusion. Given that the repulsive mean-field interactions between hadrons have a significant effect on the diffusion thermopower matrix and diffusion coefficient matrix in the baryon-rich region, we extend the investigation to include the impact of magnetic fields, analyzing the magneto-thermoelectric effect on both the diffusion coefficient matrix and the Hall-like diffusion coefficient matrix. The sensitivities of the magnetic field-dependent diffusion thermopower matrix and magneto-thermoelectric modified diffusion coefficient matrix to the choices of various transverse conditions are also studied.

I. INTRODUCTION

Relativistic heavy-ion collision experiments open up a unique portal for understanding the properties of strongly interacting matter under extreme temperatures. A wealth of experimental data from the relativistic heavy-ion collider (RHIC) [1–4] at Brookhaven National Laboratory (BNL) and in the large hadron collider (LHC) [5–10] at the European Organization for Nuclear Research (CERN) have indicated that a new deconfined state of matter – quark-gluon plasma (QGP) can be created. Meanwhile, quantum chromodynamics (QCD) serves as the fundamental theory of the strong interaction and the lattice QCD calculation has predicted a smooth crossover from QCD matter from a hadronic phase to a QGP phase can be realized as temperature (T) increases at the small or vanishing baryon chemical potential (μ_B) [11–13]. At large μ_B , calculations based on the low-energy QCD effective models, such as the (Polyakov-loop-) Nambu-Jona-Lasinio model [14–16], the (Polyakov-loop-) quark-meson model [17–20] have revealed that the QCD phase transition becomes first-order and terminates at a second-order critical endpoint

(CEP), which has sparked long-sought debate without conclusive experimental evidence yet [21]. Furthermore, the Beam Energy Scan (BES) program at RHIC [22, 23] and ongoing experimental programs at the Facility for Antiproton and Ion Research (FAIR) [24, 25] and the Nuclotron-based Ion Collider fAcility (NICA) [26, 27], are striving to unravel the properties of baryon-dense nuclear matter and search the potential signatures of the CEP in the QCD phase diagram.

In addition to the equilibrium QCD thermodynamical properties, the medium's response to perturbations around equilibrium, which is encoded in transport coefficients, plays a crucial role in describing the evolution of bulk matter created in relativistic heavy-ion collisions. The small shear viscosity to entropy density ratio (η/s) has been employed to successfully describe collective flow observables [28–31]. The bulk viscosity to entropy density ratio (ζ/s) exhibits a novel behavior near critical temperature [32–34]. Recently, electric conductivity has been utilized to extend the duration of the initial magnetic field generated in off-central heavy-ion collisions [35–37], and provide essential input for magnetohydrodynamic simulations [38, 39]. On the other hand, the diffusion coefficient, which characterizes the medium's response to inhomogeneities in the number density and is largely overlooked at the top RHIC and LHC energies, gains significance in the dynamical description of the evolution of low-energy heavy-ion collisions. Specifically, a diffusion coefficient matrix is specifically required to quantify the coupling among diffusion

* hxzhang@m.scnu.edu.cn

† shen_keming@ecut.edu.cn

‡ xiaoyx@mails.cnu.edu.cn

§ bwzhang@mail.cnu.edu.cn

currents of various conserved charges. This arises from the fact that QCD matter constituents, such as hadrons and quarks, carry multiple quantum conserved numbers, including baryon number (B), electric charge (Q), and strangeness (S). The complete diffusion coefficient matrix in both the QGP and hadron gas has been calculated within the Boltzmann kinetic theory [40–42]. The associated results reveal that the off-diagonal matrix elements are comparable in magnitude to the diagonal elements, making them crucial in the hydrodynamic simulation of low-energy nuclear collisions. Recently, A. Das et. al. have explicitly imposed the Landau-Lifshitz frame into the previous derivations [40, 41], and provided a unique expression in the hadron resonance gas model with and without excluded volume corrections [43]. In this study, we explore how repulsive interactions, incorporated via a density-dependent mean-field potential in the repulsive mean-field hadron resonance gas (RMFHRG) model, impact the diffusion properties of hadronic matter.

The thermoelectric effect, which facilitates the direct conversion of temperature differences into electric voltage and vice versa through a thermocouple, has been extensively explored across various disciplines, including material science, solid-state physics, and chemistry. The most fundamental thermoelectric effect is the Seebeck effect, which describes the generation of an electric voltage caused by a temperature gradient within a conductive material. Intriguingly, heavy-ion collisions offer a unique platform to study the Seebeck effect in QCD matter. This is due to the notable temperature difference between the central region and peripheral region of the fireball. The Seebeck coefficient or thermopower, defined as the ratio of the induced electric field and the collinear temperature gradient ($S = \mathbf{E}/\nabla T$) in the absence of electric current, has been estimated in both the partonic and hadronic phases of QCD matter [44–52]. Unlike studies in condensed matter physics, the non-zero net conserved number is required to estimate the Seebeck coefficient in QCD matter. To our best knowledge, most estimations have focused exclusively on scenarios where only net baryon density is nonzero, neglecting the potential contributions of other conserved charges to the thermoelectric effect. However, it's important to note that the gradients of multiple conserved charge chemical thermal potentials ($\nabla(\mu_q/T)$ with $q \in \{Q, B, S\}$) are also a source to generate an internal electric field, which is quantified by diffusion thermopower matrix, denoted as $M^{qQ} = \mathbf{E}/(T\nabla(\mu_q/T))$, in the limit of zero electric current. Such thermoelectric effect involving multiple conserved charges has the potential to further influence the thermally spin Hall effect (TSHE) recently proposed in the heavy-ion collisions at BES energies [53, 54]. Given that the thermoelectric effect is highly related to the gradients of conserved charge chemical potentials and can theoretically impact the diffusion coefficient matrix, to the best of our knowledge, there have been no associated studies yet. This serves as the primary motivation for our research.

Considering that a partial magnetic field created in the off-central heavy-ion collisions can persist into the hadronic phase, the motions of charged hadrons driven by $\nabla(T(\mu_q/T))$ undergo deflection. This deflection results in a transverse or Hall-like electric field, viz, $\mathbf{E} \sim \nabla(T(\mu_q/T)) \times \mathbf{H}$ in the magnetic field. This phenomenon, known as the magneto-thermoelectric effect, is quantified by the Hall-like diffusion thermopower. Similarly, additional Hall-type diffusion currents of conserved charges also arise in the magnetic field and are determined by the Hall-like diffusion coefficient matrix. Thus, the magneto-thermoelectric effect can affect both the magnetic field-dependent diffusion coefficient matrix and the Hall-like diffusion coefficient matrix. It is crucial to note that the formulation of the magneto-thermoelectric modified diffusion coefficient matrix depends on the choices of transverse conditions: 1) all transverse gradients in net conserved charge densities vanish, 2) another transverse specific conserved charge diffusion current disappears apart from a zero transverse electric current.

This paper is organized as follows. In Sec. II, we provide a brief overview of the ideal hadron resonance gas (IHRG) model and repulsive mean-field hadron resonance gas (RMFHRG) model. In Sec. III, we derive the general formulae for the diffusion thermopower and diffusion coefficient of conserved charges by solving the Boltzmann equation under relaxation time approximation in the framework of the RMFHRG model with and without magnetic field. We present, for the first time, the expressions of the magneto-thermoelectric modified diffusion coefficient matrix under various transverse conditions. Sec. IV delves into the impacts of RMF correction, baryon chemical potential, magnetic field, and (magneto-)thermoelectric effect on the (Hall-like-) diffusion coefficient matrix. We summarize our findings in Sec. V.

Throughout this paper, we adopt natural units with $c = \hbar = k_B = 1$, and work in flat Minkowski space-time with metric tensor $g^{\mu\nu} = \text{diag}(1, -1, -1, -1)$, thus the fluid velocity satisfies $u^\mu u_\mu = 1$. The tensor $\Delta^{\mu\nu} = g^{\mu\nu} - u^\mu u^\nu$ is the projection operator onto the three-dimensional subspace orthogonal to u^μ . In the local rest frame, $u^\mu = (1, \mathbf{0})$, the projector $\Delta^{\mu\nu}$ has the form: $\Delta_{\mu\nu} = \Delta^{\mu\nu} = \text{diag}(0, -1, -1, -1)$, $\Delta_\nu^\mu = \text{diag}(0, 1, 1, 1)$. The projection of any four-vector $A^\mu = (A^0, \mathbf{A})$ onto the three-dimensional subspace orthogonal to u^μ is defined as $A^{(\mu)} \equiv \Delta_\nu^{(\mu)} A^\nu$. The four-derivative is decomposed as $\partial^\mu \equiv \nabla^\mu + u^\mu D$, where $D = u^\mu \partial_\mu$ and $\nabla_\nu = \Delta_\nu^\alpha \partial_\alpha$ denote the time derivative and spatial gradient operator in the local rest frame, respectively. In the local rest frame, we have $\nabla^\mu \equiv (0, -\nabla)$.

II. MODEL DESCRIPTION

The hadron resonance gas (HRG) model [55, 56] is a simplistic thermal statistical model that successfully de-

describes the low-temperature hadronic phase of QCD at chemical freeze-out. In the IHRG model, the attractive interactions between hadrons are implicitly accounted for by including all the resonances with zero width, while the repulsive interactions among hadrons, which are already known from nucleon-nucleon scattering experiments, are missed. Consequently, several extensions of the IHRG model have emerged, such as excluded volume HRG model [57–59], van der Waals HRG model [60, 61] and repulsive mean-field HRG model [62–65]. These extensions aim to provide a more precise fit to various thermodynamic observables derived from lattice QCD simulations. In this work, we utilize the repulsive mean-field hadron resonance gas (RMFHRG) model to describe the repulsive interactions between the hadrons.

A. Ideal hadron resonance gas (IHRG) model

In the IHRG model, the partition function, containing all relevant degrees of freedom of the confined QCD phase, is the starting point for deriving thermodynamic observables. The logarithm of the total partition function in the grand canonical ensemble is given as

$$\ln Z^{id} = \sum_a \ln Z_a^{id}(T, \mu_a, m_a), \quad (1)$$

where logarithm of the partition function for hadron species a is given by

$$\ln Z_a^{id} = \pm V \sum_a \int d\Gamma_a \ln[1 \pm e^{-\beta(\epsilon_a^0 - \mu_a)}]. \quad (2)$$

Here, the superscript “ id ” represents the ideal gas and V is the system volume, we use the notation $d\Gamma_a = d_a d^3 p_a / (2\pi)^3$, where d_a is the spin degeneracy of hadron species a . $\beta = 1/T$ is the inverse temperature of the system. The front upper and lower signs correspond to (anti-)fermions and bosons, respectively. $\epsilon_a^0 = \sqrt{\mathbf{p}_a^2 + m_a^2}$ is the energy of hadron species a with mass m_a . The chemical potential of hadron species a is defined as $\mu_a(\{\mu_q\}) = B_a \mu_B + Q_a \mu_Q + S_a \mu_S$, where $\{\mu_q\} \equiv \{\mu_B, \mu_Q, \mu_S\}$ are the baryon, electric and strangeness chemical potentials, respectively, and B_a , Q_a and S_a are the corresponding quantum numbers for particle species a . Therefore, the ideal thermodynamics including total pressure (P^{id}), total energy density (\mathcal{E}^{id}), and total number density (ρ^{id}) in the IHRG model can be obtained as follows.

$$P^{id} = \sum_a P_a^{id} = \frac{\partial \ln Z^{id}}{\beta \partial V} = \sum_a \int d\Gamma_a \frac{\mathbf{p}_a^2}{3\epsilon_a^0} f_a^{id}, \quad (3)$$

$$\mathcal{E}^{id} = \sum_a \mathcal{E}_a^{id} = -\frac{1}{V} \frac{\partial \ln Z^{id}}{\partial \beta} = \sum_a \int d\Gamma_a \epsilon_a^0 f_a^{id}, \quad (4)$$

$$\rho^{id} = \sum_a \rho_a^{id} = \frac{T}{V} \frac{\partial \ln Z^{id}}{\partial \mu_a} = \sum_a \int d\Gamma_a f_a^{id}. \quad (5)$$

Here, f_a^{id} is the thermal equilibrium distribution function of particle species a in the IHRG model. It is expressed as

$$f_a^{id}(T, \mu_a) = [\exp[(\epsilon_a^0 - \mu_a)\beta] \pm 1]^{-1}, \quad (6)$$

where the signs \pm correspond to the Fermi-Dirac and Bose-Einstein statistics, respectively.

B. Repulsive mean-field hadron resonance gas (RMFHRG) model

The RMFHRG model is an extension of the IHRG model that includes short-range repulsive interactions between hadrons via a mean-field approach. In this model, the single-particle energy is modified as [66]

$$\tilde{\epsilon}_a = \epsilon_a^0 + U_a, \quad (7)$$

where U_a is the potential describing the repulsive interactions between hadrons, and acts as an additional chemical potential. In the RMFHRG model, the repulsive interactions only among meson-meson pairs, baryon-baryon pairs, and antibaryon-antibaryon pairs are considered [64]. The mean-field potentials for (anti-)baryons and mesons are defined as [64, 66]

$$U_{a \in \{B, \bar{B}\}}(\rho_{B, \bar{B}}) = K_B \rho_{B, \bar{B}}, \quad U_{a \in \{M\}}(\rho_M) = K_M \rho_M, \quad (8)$$

with subscripts B , \bar{B} , M denoting baryons, antibaryons, and mesons, respectively, $\rho_{B, \bar{B}, M}$ are the respective total number densities. Two phenomenological parameters K_M and K_B are introduced to scale the repulsive interaction strength among the mesons and (anti-)baryons, respectively. Accordingly, the logarithm of the total partition function in the RMFHRG model can be expressed as

$$\ln Z^{\text{RMF}} = \pm V \sum_a \int d\Gamma_a \ln[1 \pm e^{-\beta(\epsilon_a^0 - \mu_a^*)}] - V \beta \chi_{a \in \{M, B, \bar{B}\}}(\rho_{M, B, \bar{B}}) \quad (9)$$

where the effective chemical potential of hadron species a is defined as $\mu_a^* = \sum_q q_a \mu_q - K_{B, \bar{B}} \rho_{B, \bar{B}}$ for (anti-)baryons, and $\mu_a^* = \sum_q q_a \mu_q - K_M \rho_M$ for mesons. In the RMFHRG model, $\rho_{B, \bar{B}, M}$ are calculated as follows:

$$\rho_{B, \bar{B}, M} = \sum_{a \in \{B, \bar{B}, M\}} \int d\Gamma_a \tilde{f}_a^0. \quad (10)$$

Here, \tilde{f}_a^0 represents the thermal equilibrium distribution function of particle species a in the RMFHRG model. It is given by:

$$\tilde{f}_a^0(T, \mu_a) = f_a^{id}(T, \mu_a^*) = [\exp[(\epsilon_a^0 - \mu_a^*)\beta] \pm 1]^{-1}. \quad (11)$$

In Eq. (9), χ_a is an additional correction factor to avoid the double counting of the mean-field potential

and to ensure the correct number density per particle $\rho_a = \frac{T}{V} \frac{\partial \ln Z^{\text{RMF}}}{\partial \mu_a}$ (or the correct energy density per particle $\mathcal{E}_a = \partial \mathcal{E} / \partial \rho_a$). Assuming that hadron species a is a baryon or antibaryon, its number density takes the following form:

$$\rho_a = \rho_a - \rho_a \left(\frac{\partial U_a}{\partial \rho_{B,\bar{B}}} \frac{\partial \rho_{B,\bar{B}}}{\partial \mu_a} \right) - \frac{\partial \chi_a}{\partial \rho_{B,\bar{B}}} \frac{\partial \rho_{B,\bar{B}}}{\partial \mu_a}. \quad (12)$$

Accordingly, the expression of χ_a can be obtained as

$$\chi_{a \in \{B, \bar{B}\}}(\rho_{B, \bar{B}}) = -\frac{1}{2} K_B \rho_{B, \bar{B}}^2. \quad (13)$$

Similarly, if hadron species a is a meson, $\chi_{a \in \{M\}}(\rho_M) = -\frac{1}{2} K_M \rho_M^2$. By utilizing Eqs. (3-4) along with Eq. (9), we can derive the pressure and energy density for baryons, antibaryons, and mesons in the RMFHRG model, which are expressed respectively as

$$P_{B, \bar{B}, M} = \sum_{a \in \{B, \bar{B}, M\}} P_a^{id}(T, \mu_a^*) - \chi_{B, \bar{B}, M}(\rho_{B, \bar{B}, M}), \quad (14)$$

$$\mathcal{E}_{B, \bar{B}, M} = \sum_{a \in \{B, \bar{B}, M\}} \mathcal{E}_a^{id}(T, \mu_a^*) + \chi_{B, \bar{B}, M}(\rho_{B, \bar{B}, M}). \quad (15)$$

The total pressure and total energy density in the RMFHRG model are given by $P = P_B + P_{\bar{B}} + P_M$ and $\mathcal{E} = \mathcal{E}_B + \mathcal{E}_{\bar{B}} + \mathcal{E}_M$, respectively. Compared to the IHRG model, the RMFHRG model incorporates an additional term in both pressure and energy density, ensuring the thermodynamic consistency. In the present RMFHRG model, all distinct (anti-)baryons or mesons are assigned a uniform repulsive interaction strength. Specifically, $K_B = 0.45 \text{ GeV} \cdot \text{fm}^3$ and $K_M = 0.05 \text{ GeV} \cdot \text{fm}^3$ are adopted to improve the agreement with the thermodynamic quantities obtained from the lattice QCD simulations at zero and finite baryon densities [64, 65].

III. THERMOELECTRIC COEFFICIENTS AND DIFFUSION COEFFICIENTS OF CONSERVED CHARGES IN BOLTZMANN KINETIC THEORY

A. Formalism

It is effective to calculate the transport coefficients of hadronic matter within the kinetic theory framework. The evolution of the single-particle phase-space distribution function $f_a(x, p_a)$ can be described by the Boltzmann equation within the covariant formalism [67],

$$p_a^\mu \partial_\mu f_a(x, p_a) + m_a K^\mu \partial_\mu^{(p)} f_a(x, p_a) = \mathcal{C}_a[f_a], \quad (16)$$

where $p_a^\mu = (\epsilon_a^0, \mathbf{p}_a)$ represents the four-momentum of the particle species a , K^μ is the four-force experienced by individual particle, and $\mathcal{C}_a[f_a]$ denotes the collision

term. When a particle is subjected to an electromagnetic field force, then $K_a^\mu = -\epsilon_a^0 \partial^\mu U_a(x)/m_a + \frac{Q_a}{m_a} p_{a\nu} F^{\mu\nu}$. Here, U_a refers to the repulsive mean-field potential among hadrons, and $F^{\mu\nu}$ is the electromagnetic field-strength tensor. This tensor is defined as: $F^{\mu\nu} \equiv E^\mu u^\nu - E^\nu u^\mu + \frac{1}{2} \epsilon^{\mu\nu\alpha\beta} (u_\alpha H_\beta - u_\beta H_\alpha)$, where $\epsilon^{\mu\nu\alpha\beta}$ is the totally anti-symmetric Levi-Civita tensor. The four-vectors $E^\mu \equiv F^{\mu\nu} u_\nu$ and $H^\mu \equiv \epsilon^{\mu\nu\alpha\beta} F_{\nu\alpha} u_\beta / 2$ are nothing but the electric and magnetic fields measured in the frame where the fluid moves with a velocity u^μ . Both $E^\mu = (0, \mathbf{E})$ and $H^\mu = (0, \mathbf{H})$ are space like, satisfying $E^\mu u_\mu = 0, H^\mu u_\mu = 0$. They can be normalized as $E^\mu E_\mu = -E^2, H^\mu H_\mu = -H^2$, where $E \equiv |\mathbf{E}|$ and $H \equiv |\mathbf{H}|$. Note that in this study, the electric field is induced by gradients of conserved charge densities rather than a decaying external magnetic field.

Considering that the system is slightly deviated from the local equilibrium, the phase space distribution function for hadron species a can be formulated as:

$$f_a = \bar{f}_a^0 (1 + \phi_a), \quad (17)$$

where the deviation function $|\phi_a| \ll 1$. Here, \bar{f}_a^0 represents the local equilibrium distribution function within the RMFHRG model, given by

$$\bar{f}_a^0 = [\exp((p_a^\mu u_\mu + U_a)\beta - \sum_q q_a \alpha_q) + 1]^{-1}, \quad (18)$$

with $\alpha_q \equiv \mu_q \beta$ denoting the chemical thermal potential of conserved charge q .

To solve Eq. (16), the deviation function ϕ_a is assumed have the following linear combination form:

$$\phi_a \approx - \sum_q \mathcal{B}_a^q p_a^\mu \nabla_\mu \alpha_q - \mathcal{G}_a p_a^\mu \beta E_\mu + \dots, \quad (19)$$

where \mathcal{B}_a^q and \mathcal{G}_a are unknown functions with respect to momentum p_a . For the binary inelastic or reactive collisions $a(p_a) + b(p_b) \rightarrow c(p_c) + d(p_d)$, the initial particle species (a, b) are allowed to be different from final particles species (c, d), such that the collision term in Eq. (16) reads as [68–70]

$$\begin{aligned} \mathcal{C}_a = & \frac{1}{2} \sum_{b, c, d} \int d\Gamma'_b d\Gamma''_c d\Gamma'''_d [W_{ab|cd}(p_a, p'_b | p''_c, p'''_d) \\ & \times f''_c f'''_d (1 + t_a f_a)(1 + t_b f'_b) - W_{cd|ab}(p''_c, p'''_d | p_a, p'_b) \\ & \times f_a f'_b (1 + t_c f''_c)(1 + t_d f'''_d)], \end{aligned} \quad (20)$$

where $(1 + t_a f_a)$ with $t_a = \pm$ correspond to Bose enhancement factor and Pauli blocking factor, respectively. Here, $W_{ab|cd}(p_a, p'_b | p''_c, p'''_d)$ is collisional transition rate, in the absence of a reaction threshold, it satisfies the detailed balance property [68]

$$W_{ab|cd}(p_a, p'_b | p''_c, p'''_d) = W_{cd|ab}(p''_c, p'''_d | p_a, p'_b). \quad (21)$$

Futhermore, the transition rate remains invariant under the interchange of momenta of incoming or outgoing

particles: $W_{ab|cd}(p_a, p'_b|p''_c, p'''_d) = W_{ba|cd}(p'_b, p_a|p''_c, p'''_d) = W_{ab|dc}(p_a, p'_b|p''_c, p'''_d) = W_{ba|dc}(p'_b, p_a|p''_c, p'''_d)$. The prefactor $1/2$ in Eq. (20) is added to correct the double counting from the symmetry under the exchange of the momenta of the final state p''_c and p'''_d . By utilizing the detailed balance condition, for example, $a + b \leftrightarrow c + d$ gives $\bar{f}_c^{0''} \bar{f}_d^{0'''}(1+t_a \bar{f}_a^0)(1+t_b \bar{f}_b^{0'}) = \bar{f}_a^0 \bar{f}_b^{0'}(1+t_c \bar{f}_c^{0''})(1+t_d \bar{f}_d^{0'''})$, then the collision term is computed as

$$\begin{aligned} C_a &= \frac{1}{2} \int d\Gamma'_b d\Gamma''_c d\Gamma'''_d W_{ab|cd}(p_a, p'_b|p''_c, p'''_d) \\ &\quad \times \{ \bar{f}_a^0 \bar{f}_b^{0'} [(1+t_d \bar{f}_d^{0''''}) \phi''_c + (1+t_c \bar{f}_c^{0''}) \phi'''_d] \\ &\quad - \bar{f}_c^{0''} \bar{f}_d^{0''''} [(1+t_b \bar{f}_b^{0'}) \phi_a + (1+t_a \bar{f}_a^0) \phi'_b] \} \end{aligned} \quad (22)$$

$$\begin{aligned} &= -\frac{1}{2} \int d\Gamma'_b d\Gamma''_c d\Gamma'''_d W_{ab|cd}(p_a, p'_b|p''_c, p'''_d) \\ &\quad \times \frac{\bar{f}_a^0 \bar{f}_b^{0'} (1+t_c \bar{f}_c^{0''})}{(1+t_a \bar{f}_a^0)} (1+t_d \bar{f}_d^{0''''}) \phi_a. \end{aligned} \quad (23)$$

Here, we have assumed that particle species a is slightly out of equilibrium ($\phi_a \neq 0$), while all other particles are in equilibrium ($\phi'_b = \phi''_c = \phi'''_d = 0$). In this study, our focus is solely on elastic binary collisions. The transition rate in the elastic limit is defined as [68]:

$$W_{ab|cd} = \gamma_{ab} (\delta_{ac} \delta_{bd} + \delta_{ad} \delta_{bc}) W_{ab}, \quad (24)$$

where γ_{ab} has been inserted to guarantee that W_{ab} represents the transition rate both for the case of identical particle species ($a = b$) and particles of different species ($a \neq b$). Accordingly, the collision term for the elastic binary process $a(p_a) + b(p'_b) \rightarrow a(p''_a) + b(p'''_b)$ is formulated as

$$\begin{aligned} C_a &= -\sum_b \gamma_{ab} \int d\Gamma'_b d\Gamma''_a d\Gamma'''_b W_{ab}(p_a, p'_b|p''_a, p'''_b) \\ &\quad \times \frac{\bar{f}_a^0 \bar{f}_b^{0'} (1+t_a \bar{f}_a^{0''})}{(1+t_a \bar{f}_a^0)} (1+t_b \bar{f}_b^{0''''}) \phi_a. \end{aligned} \quad (25)$$

We shall now consider the collision term in Eq. (16) using a simple and popular approximation, known as the relaxation time approximation (RTA) [71]. Under the RTA, the collision term takes the form:

$$-\frac{\epsilon_a^0 \bar{f}_a^0 \phi_a}{\tau_a} = C_a = -\frac{\epsilon_a^0 \delta f_a}{\tau_a}. \quad (26)$$

Here, τ_a denotes the relaxation time of hadron species a , describing how fast the system reaches the equilibrium again. The term $\delta f_a = f_a - \bar{f}_a^0$ is a perturbation term. Then, the energy-momentum tensor $T^{\mu\nu}$ and the net conserved charge four-current N_q^μ can be expressed in terms of the phase space distribution function as follows:

$$T^{\mu\nu} = \sum_a \int d\Gamma_a \frac{p_a^\mu p_a^\nu}{\epsilon_a^0} f_a + g^{\mu\nu} \chi_a, \quad (27)$$

$$N_q^\mu = \sum_a q_a \int d\Gamma_a \frac{p_a^\mu}{\epsilon_a^0} f_a, \quad (28)$$

where $p_a^{*\mu} = p_a^\mu + U_a^\mu$. In a non-equilibrium system, the energy-momentum diffusion four-current and the conserved charge diffusion four-current are defined as $W^\mu \equiv \Delta_\nu^\mu T^{\alpha\nu} u_\alpha$ and $V_q^\mu \equiv \Delta_\nu^\mu N_q^\nu$, respectively [72, 73]. They can also be expressed as:

$$W^\mu = \sum_a \int d\Gamma_a \frac{\Delta_\nu^\mu p_a^\nu (\epsilon_a^0 + U_a)}{\epsilon_a^0} \bar{f}_a^0 \phi_a, \quad (29)$$

$$V_q^\mu = \sum_a q_a \int d\Gamma_a \frac{\Delta_\nu^\mu p_a^\nu}{\epsilon_a^0} \bar{f}_a^0 \phi_a. \quad (30)$$

In ideal hydrodynamics, the fluid four-velocity is determined because the energy and conserved charge number currents are parallel to each other. The local rest frame of the fluid is then defined by the requirement that these currents vanish identically. However, in dissipative hydrodynamics, the energy flow and charge number flow are separate, leading to a non-unique definition of the fluid four-velocity [74]. There are two natural choices for fixing the local rest frame of fluid: Eckart frame (or conserved charge frame) and Landau-Lifshitz frame (or energy frame). In the Eckart frame, the fluid velocity is parallel to one of the conserved charge currents, demanding the overall diffusion current of that conserved charge to be zero. However, in low-energy heavy-ion collisions, there are multiple conserved charges and are not necessarily non-vanishing in all regions of space-time, therefore, the definition of Eckart frame may not be suitable [72]. On the other hand, in the Landau-Lifshitz frame, the fluid velocity is parallel to the energy flow, requiring the total energy-momentum diffusion current to vanish in the local rest frame. The Landau-Lifshitz frame is our choice for the local rest frame of fluid.

Upon substitution of Eq. (26) into the right-hand side of Eq. (16), we can compute the perturbation term δf_a for the first-order gradient expansion as follows:

$$\begin{aligned} \delta f_a &= \frac{\tau_a}{\epsilon_a^0} \bar{f}_a^0 (1 - \bar{f}_a^0) \left[p_a^\mu p_a^\nu \beta (u_\mu D u_\nu + \nabla_\mu u_\nu) \right. \\ &\quad + p_a^\mu (p_a \cdot u + U_a) (u_\mu D \beta + \nabla_\mu \beta) \\ &\quad - p_a^\mu \sum_q q_a (u_\mu D \alpha_q + \nabla_\mu \alpha_q) \\ &\quad + p_a^\mu \beta (u_\mu D U_a + \nabla_\mu U_a) - p_a^\mu \beta (u_\mu D U_a + \nabla_\mu U_a) \\ &\quad \left. + Q_a \beta p_{a\nu} F^{\mu\nu} u_\mu \right]. \end{aligned} \quad (31)$$

In ideal hydrodynamics, taking the projection of $\partial_\mu T^{\mu\nu} = 0$ along the direction orthogonal to u_ν , one gets $u_\nu \partial_\mu T^{\mu\nu} = u_\nu [D \mathcal{E} u^\nu + (\mathcal{E} + P) \theta u^\nu + (\mathcal{E} + P) D u^\nu - \nabla^\nu P] = 0$, where θ is the expansion rate. Due to $u_\nu u^\nu = 1$, we have $u_\nu \partial_\mu u^\nu = 0$. Then we can derive $D u_\mu = \frac{1}{\omega} \nabla_\mu P$ with ω being enthalpy density. Recalling the Gibbs-Duhem relation, $dP = s dT + \sum_q n_q d\mu_q$, one arrives at: $\nabla_\mu P = -\beta^{-1} \omega \nabla_\mu \beta + \beta^{-1} \sum_q n_q \nabla_\mu \alpha_q$, where n_q is conserved net charge density. By invoking momentum conservation $\nabla_\mu P = 0$, we ultimately obtain: $\nabla_\mu \beta = \sum_q \frac{n_q}{\omega} \nabla_\mu \alpha_q$.

B. For vanishing magnetic field

In Eq. (31), we first consider only spatial-dependent gradient terms and neglect the magnetic field effect, δf_a can be simplified to:

$$\delta f_a = \frac{\tau_a}{\epsilon_a^0} \bar{f}_a^0 (1 - \bar{f}_a^0) \left[p_a^\mu p_a^\nu \beta \nabla_\mu u_\nu - Q_a \beta p_{a\nu} E^\nu + p_a^\mu \sum_q \left((p_a \cdot u + U_a) \frac{n_q}{\omega} - q_a \right) \nabla_\mu \alpha_q \right]. \quad (32)$$

We only retain the terms related to the conserved charge diffusion current, the above equation can be further reduced as

$$\delta f_a \simeq -\tau_a \frac{p_a^\mu}{\epsilon_a^0} F_a Q_a E_\mu + \sum_q \tau_a \frac{p_a^\mu}{\epsilon_a^0} H_a^q \nabla_\mu \alpha_q. \quad (33)$$

The functions of F_a and H_a^q in Eq. (33) are defined as follows:

$$F_a = \beta \bar{f}_a^0 (1 \pm \bar{f}_a^0), \quad (34)$$

$$H_a^q = \left(\frac{n_q}{\omega} (\epsilon_a^0 + U_a) - q_a \right) \bar{f}_a^0 (1 \pm \bar{f}_a^0). \quad (35)$$

In the Landau-Lifshitz frame condition, the the total energy-momentum diffusion current is required to vanish, i.e., $W^\mu = 0$. By inserting Eq. (19) into Eq. (29), one gets

$$\sum_a \int d\Gamma_a \tilde{\epsilon}_a \frac{p_a^{(\mu)} p_a^{(\nu)}}{\epsilon_a^0} \left[\sum_q \mathcal{B}_{a,\text{part}}^q \nabla_\nu \alpha_q + \mathcal{G}_a \beta E_\nu \right] \bar{f}_a^0 = 0. \quad (36)$$

Given that we have the particular solutions $\mathcal{B}_{a,\text{part}}^q$, $\mathcal{G}_{a,\text{part}}$, other solutions can be expressed as $\mathcal{B}_a^q = \mathcal{B}_{a,\text{part}}^q - b^q$ and $\mathcal{G}_a = \mathcal{G}_{a,\text{part}} - g$, respectively, where b^q and g are the constants independent of particle species a . Inserting these expressions into Eq. (36) to determine the uniqueness of solutions, we arrive at:

$$\begin{aligned} & \sum_a \int d\Gamma_a \tilde{\epsilon}_a \frac{p_a^{(\mu)} p_a^{(\nu)}}{\epsilon_a^0} \left[\sum_q \mathcal{B}_{a,\text{part}}^q \nabla_\nu \alpha_q + \mathcal{G}_{a,\text{part}} \beta E_\nu \right] \bar{f}_a^0 \\ &= \sum_a \int d\Gamma_a \tilde{\epsilon}_a \frac{p_a^{(\mu)} p_a^{(\nu)}}{\epsilon_a^0} \left[\sum_q b^q \nabla_\nu \alpha_q + g \beta E_\nu \right] \bar{f}_a^0. \end{aligned} \quad (37)$$

Employing the identity $3T\omega = \sum_a \int d\Gamma_a (\epsilon_a^0 + U_a) \frac{p_a^2}{\epsilon_a^0} \bar{f}_a^0$, and comparing the coefficients of $\nabla_\nu \alpha_q$ and βE_ν , we get

$$b^q = \frac{1}{3T\omega} \sum_a \int d\Gamma_a (\epsilon_a^0 + U_a) \frac{p_a^2}{\epsilon_a^0} \mathcal{B}_{a,\text{part}}^q \bar{f}_a^0, \quad (38)$$

$$g = \frac{1}{3T\omega} \sum_a \int d\Gamma_a (\epsilon_a^0 + U_a) \frac{p_a^2}{\epsilon_a^0} \mathcal{G}_{a,\text{part}} \bar{f}_a^0. \quad (39)$$

Inserting Eq. (19) into Eq. (30), and utilizing Eqs. (38-39), the diffusion current of conserved charge q' can be

written as

$$V_{q'}^\mu = \sum_a q'_a \int d\Gamma_a \frac{p_a^{(\mu)} p_a^{(\nu)}}{\epsilon_a^0} \left[- \sum_q (\mathcal{B}_{a,\text{part}}^q - b^q) \nabla_\nu \alpha_q - (\mathcal{G}_{a,\text{part}} - g) \beta E_\nu \right] \bar{f}_a^0 \quad (40)$$

$$= - \sum_a q'_a \int d\Gamma_a \frac{p_a^{(\mu)} p_a^{(\nu)}}{\epsilon_a^0} \left[\sum_q \mathcal{B}_{a,\text{part}}^q \nabla_\nu \alpha_q + \mathcal{G}_{a,\text{part}} \beta E_\nu \right] \bar{f}_a^0 - n'_{q'} T \sum_b b^q \nabla^\mu \alpha_q - g n'_{q'} E^\mu, \quad (41)$$

where the orthogonality relation of $p_a^{(\mu)}$: $p_a^{(\mu)} p_a^{(\nu)} = \frac{\Delta^{\mu\nu}}{3} p_a^{(\gamma)} p_{a(\gamma)} = -\frac{p_a^2}{3} \Delta^{\mu\nu}$ and the identity $\sum_a \int q'_a d\Gamma_a \frac{p_a^2}{3\epsilon_a^0} \bar{f}_a^0 = n_{q'} T$ have been employed. By substituting Eq. (38) and Eq. (39) into Eq. (41), we derive:

$$\begin{aligned} V_{q'}^\mu &= - \sum_a q'_a \int d\Gamma_a \frac{p_a^{(\mu)} p_a^{(\nu)}}{\epsilon_a^0} \left[\sum_q \mathcal{B}_{a,\text{part}}^q \nabla_\nu \alpha_q + \mathcal{G}_{a,\text{part}} \beta E_\nu \right] \bar{f}_a^0 \\ &+ \sum_{a'} \frac{n_{q'}}{\omega} \int d\Gamma_{a'} \tilde{\epsilon}_{a'} \frac{p_{a'}^{(\mu)} p_{a'}^{(\nu)}}{\epsilon_{a'}^0} \sum_q \mathcal{B}_{a',\text{part}}^q \bar{f}_{a'}^0 \nabla_\nu \alpha_q \\ &+ \frac{n_{q'}}{\omega T} \sum_{a'} \int d\Gamma_{a'} \tilde{\epsilon}_{a'} \frac{p_{a'}^{(\mu)} p_{a'}^{(\nu)}}{\epsilon_{a'}^0} \mathcal{G}_{a',\text{part}} \bar{f}_{a'}^0 E_\nu. \end{aligned} \quad (42)$$

Here, we emphasize that both the \sum_a and $\sum_{a'}$ represent the summation over all the hadron species under consideration. Thus, we can combine these distinct summation indices into a single summation index: $\sum_a A_a + \sum_{a'} B_{a'} = \sum_a (A_a + B_a)$. Accordingly, the above equation can be further simplified to:

$$V_{q'}^\mu = \sum_a \int d\Gamma_a \frac{p_a^{(\mu)} p_a^{(\nu)}}{\epsilon_a^0} \left[\frac{n_{q'} (\epsilon_a^0 + U_a)}{\omega} - q'_a \right] \times \left[\sum_q \mathcal{B}_{a,\text{part}}^q \nabla_\nu \alpha_q + \beta \mathcal{G}_{a,\text{part}} E_\nu \right] \bar{f}_a^0. \quad (43)$$

We replace the right-hand side of Eq. (26) with Eq. (33), and insert ϕ_a from Eq. (19) into the left-hand side of Eq. (26). By equating δf_a and $\bar{f}_a^0 \phi_a$ through matching tensor structure, we can derive the particular solutions for the functions \mathcal{B}_a^q and \mathcal{G}_a from ϕ_a , which are presented as follows:

$$\mathcal{B}_{a,\text{part}}^q = \frac{\tau_a}{\epsilon_a^0} \left[q_a - \frac{n_q}{\omega} (\epsilon_a^0 + U_a) \right] (1 \pm \bar{f}_a^0), \quad (44)$$

$$\mathcal{G}_{a,\text{part}} = Q_a \frac{\tau_a}{\epsilon_a^0} (1 \pm \bar{f}_a^0). \quad (45)$$

According to the linear response theory, Eq. (43) can

be expressed in the following matrix form:

$$\begin{bmatrix} V_B^\mu \\ V_Q^\mu \\ V_S^\mu \end{bmatrix} = \begin{bmatrix} \eta^{BQ} \\ \eta^{QQ} \\ \eta^{SQ} \end{bmatrix} E^\mu + \begin{bmatrix} \kappa^{BB} & \kappa^{QB} & \kappa^{SB} \\ \kappa^{BQ} & \kappa^{QQ} & \kappa^{SQ} \\ \kappa^{BS} & \kappa^{QS} & \kappa^{SS} \end{bmatrix} \begin{bmatrix} \nabla^\mu \alpha_B \\ \nabla^\mu \alpha_Q \\ \nabla^\mu \alpha_S \end{bmatrix}. \quad (46)$$

The diffusion coefficient matrix, $\kappa^{qq'}$ ($q, q' \in \{B, Q, S\}$), which quantifies the coupling between the diffusion of various conserved charges, is expressed as

$$\begin{aligned} \kappa^{qq'} &= \sum_a \frac{d_a}{3} \int \frac{d^3 p_a}{(2\pi)^3} \tau_a \frac{\mathbf{p}_a^2}{(\epsilon_a^0)^2} \left[q'_a - (\epsilon_a^0 + U_a) \frac{n'_q}{\omega} \right] \\ &\times \left[q_a - (\epsilon_a^0 + U_a) \frac{n_q}{\omega} \right] \bar{f}_a^0 (1 \pm \bar{f}_a^0). \end{aligned} \quad (47)$$

This expression is equivalent to the one presented in Ref. [43], excluding the effects of quantum statistics and the repulsive mean-field interactions. In Eq. (46), the thermoelectric transport coefficient matrix, $\eta^{qq'}$, is defined as

$$\begin{aligned} \eta^{qq'} &= \sum_a \frac{d_a \beta}{3} \int \frac{d^3 p_a}{(2\pi)^3} \tau_a \frac{\mathbf{p}_a^2}{(\epsilon_a^0)^2} q'_a \\ &\times \left[q_a - (\epsilon_a^0 + U_a) \frac{n_q}{\omega} \right] \bar{f}_a^0 (1 \pm \bar{f}_a^0). \end{aligned} \quad (48)$$

By setting $q'_a = Q_a$, we redefine η^{qQ} as the thermoelectric conductivity associated with the conserved charge q . When the net electric diffusion current vanishes, i.e., $V_Q^i = V_Q = 0$, the induced electric field is given by:

$$\mathbf{E} = \sum_q M^{qQ} T \nabla \alpha_q. \quad (49)$$

Here, M^{qQ} is defined as diffusion thermopower associated with the conserved charge q , which quantifies the ability of hadronic matter to convert the gradients in conserved charge chemical thermal potentials into an electric field, and it is expressed as:

$$M^{qQ} = \beta \kappa^{qQ} / \eta^{QQ}. \quad (50)$$

By inserting Eq. (49) into Eq. (46), Eq. (43) can be rewritten as

$$\begin{bmatrix} V_B^\mu \\ V_Q^\mu \\ V_S^\mu \end{bmatrix} = \begin{bmatrix} \tilde{\kappa}^{BB} & \tilde{\kappa}^{QB} & \tilde{\kappa}^{SB} \\ \tilde{\kappa}^{BQ} & \tilde{\kappa}^{QQ} & \tilde{\kappa}^{SQ} \\ \tilde{\kappa}^{BS} & \tilde{\kappa}^{QS} & \tilde{\kappa}^{SS} \end{bmatrix} \begin{bmatrix} \nabla^\mu \alpha_B \\ \nabla^\mu \alpha_Q \\ \nabla^\mu \alpha_S \end{bmatrix}. \quad (51)$$

In this formulation, the thermoelectric modified diffusion coefficients in the electric current sector vanish, specifically, $\tilde{\kappa}^{BQ} = \tilde{\kappa}^{SQ} = \tilde{\kappa}^{QQ} = 0$. The thermoelectric modified diffusion coefficient matrix elements in the baryon and strangeness diffusion current sectors takes the form:

$$\tilde{\kappa}^{qq''} = \kappa^{qq''} - T M^{qQ} \eta^{q''Q}. \quad (52)$$

Here, $q'' \in \{B, S\}$.

C. For finite magnetic field

Next, we investigate the influence of the magnetic field on the thermoelectric effect and diffusion processes involving multiple conserved charges in the hadronic medium. In the presence of a weak magnetic field, the field is not the dominant energy scale and its impact manifest primarily at the classical level through the cyclotron motion of charged particles. We reasonably propose that the scattering mechanism of the constituents and the thermodynamic quantities remain unaffected by the magnetic field. In the uniform electric field \mathbf{E} and external magnetic field \mathbf{H} ($\mathbf{E} \perp \mathbf{H} \perp \nabla \alpha_q$), taking into account a time-independent phase space distribution function, Eq. (16) can be reformulated as follows:

$$\mathbf{v}_a \cdot \nabla f_a + [Q_a (\mathbf{E} + \mathbf{v}_a \times \mathbf{H}) - \nabla U_a] \cdot \frac{\partial f_a}{\partial \mathbf{p}_a} = -\frac{\delta f_a}{\tau_a}. \quad (53)$$

where the RTA has been employed, and $\mathbf{v}_a \equiv \frac{d\epsilon_a^0}{d\mathbf{p}_a} = \mathbf{p}_a / \epsilon_a^0$ is the three-velocity of particle species a . Neglecting any second-order terms in δf_a , Eq. (53) can be simplified as

$$\begin{aligned} \frac{f_a}{\tau_a} + Q_a \mathbf{v}_a \times \mathbf{H} \cdot \frac{\partial f_a}{\partial \mathbf{p}_a} &= -Q_a \mathbf{E} \cdot \frac{\partial \bar{f}_a^0}{\partial \mathbf{p}_a} - (\mathbf{v}_a \cdot \nabla \bar{f}_a^0) \\ &+ \frac{\bar{f}_a^0}{\tau_a} + \nabla U_a \cdot \frac{\partial \bar{f}_a^0}{\partial \mathbf{p}_a}. \end{aligned} \quad (54)$$

We further assume the solution to Eq. (54) satisfies the following linear form:

$$\begin{aligned} f_a &= \bar{f}_a^0 - \tau_a Q_a \mathbf{E} \cdot \frac{\partial \bar{f}_a^0}{\partial \mathbf{p}_a} - \Xi \cdot \frac{\partial \bar{f}_a^0}{\partial \mathbf{p}_a} - \tau_a \mathbf{v}_a \cdot \nabla \bar{f}_a^0 \\ &+ \tau_a \nabla U_a \cdot \frac{\partial \bar{f}_a^0}{\partial \mathbf{p}_a}, \end{aligned} \quad (55)$$

where Ξ is an unknown quantity related to the magnetic field. By inserting Eq. (55) into Eq. (54), we derive:

$$\begin{aligned} -\frac{\Xi}{\tau_a} \cdot \frac{\partial \bar{f}_a^0}{\partial \mathbf{p}_a} + Q_a \mathbf{v}_a \times \mathbf{H} \cdot \frac{\partial}{\partial \mathbf{p}_a} \left[\bar{f}_a^0 - \tau_a Q_a \mathbf{E} \cdot \frac{\partial \bar{f}_a^0}{\partial \mathbf{p}_a} \right] \\ - \Xi \cdot \frac{\partial \bar{f}_a^0}{\partial \mathbf{p}_a} - \tau_a \mathbf{v}_a \cdot \nabla \bar{f}_a^0 + \tau_a \nabla U_a \cdot \frac{\partial \bar{f}_a^0}{\partial \mathbf{p}_a} = 0. \end{aligned} \quad (56)$$

To facilitate the calculation, we provide the following identities,

$$\frac{\partial \bar{f}_a^0}{\partial \mathbf{p}_a} = -\bar{f}_a^0 (1 \pm \bar{f}_a^0) \beta \mathbf{v}_a, \quad (57)$$

$$\frac{\partial \bar{f}_a^0 (1 \pm \bar{f}_a^0)}{\partial \mathbf{p}_a} = -(1 \pm 2\bar{f}_a^0) \bar{f}_a^0 (1 \pm \bar{f}_a^0) \beta \mathbf{v}_a, \quad (58)$$

$$\frac{\partial (\epsilon_a^0)^{-1}}{\partial \mathbf{p}_a} = -\frac{\mathbf{v}_a}{(\epsilon_a^0)^2}. \quad (59)$$

Then, several terms in Eq. (56) can be calculated as

$$\begin{aligned} \frac{\partial}{\partial \mathbf{p}_a} \left[\mathbf{E} \cdot \frac{\partial \bar{f}_a^0}{\partial \mathbf{p}_a} \right] &= \left[(\mathbf{E} \cdot \mathbf{v}_a)(1 \pm 2\bar{f}_a^0)\bar{f}_a^0(1 \pm \bar{f}_a^0)\mathbf{v}_a\beta^2 \right. \\ &\quad - \mathbf{E}\bar{f}_a^0(1 \pm \bar{f}_a^0)\frac{\beta}{\epsilon_a^0} \\ &\quad \left. + (\mathbf{E} \cdot \mathbf{v}_a)\bar{f}_a^0(1 \pm \bar{f}_a^0)\frac{\mathbf{v}_a}{\epsilon_a^0}\beta \right], \quad (60) \end{aligned}$$

$$\begin{aligned} \frac{\partial}{\partial \mathbf{p}_a} \left[\boldsymbol{\Xi} \cdot \frac{\partial \bar{f}_a^0}{\partial \mathbf{p}_a} \right] &= \left[(\boldsymbol{\Xi} \cdot \mathbf{v}_a)(1 \pm 2\bar{f}_a^0)\bar{f}_a^0(1 \pm \bar{f}_a^0)\mathbf{v}_a\beta^2 \right. \\ &\quad - \boldsymbol{\Xi}\bar{f}_a^0(1 \pm \bar{f}_a^0)\frac{\beta}{\epsilon_a^0} \\ &\quad \left. + (\boldsymbol{\Xi} \cdot \mathbf{v}_a)\bar{f}_a^0(1 \pm \bar{f}_a^0)\frac{\mathbf{v}_a}{\epsilon_a^0}\beta \right], \quad (61) \end{aligned}$$

$$\begin{aligned} \frac{\partial}{\partial \mathbf{p}_a} [\mathbf{v}_a \cdot \nabla \bar{f}_a^0] &= \left[\sum_q \left(\frac{n_q}{\omega}(\epsilon_a^0 + U_a) - q_a \right) \mathbf{v}_a \cdot \nabla \alpha_q \right. \\ &\quad \left. + \beta \mathbf{v}_a \cdot \nabla U_a \right] \bar{f}_a^0(1 \pm \bar{f}_a^0) \\ &\quad \times \left[(1 \pm 2\bar{f}_a^0)\beta \mathbf{v}_a - \frac{1}{\epsilon_a^0} + \frac{\mathbf{v}_a}{\epsilon_a^0} \right] \\ &\quad - (\mathbf{v}_a \cdot \nabla \beta) \mathbf{v}_a \bar{f}_a^0(1 \pm \bar{f}_a^0), \quad (62) \end{aligned}$$

$$\begin{aligned} \frac{\partial}{\partial \mathbf{p}_a} \left[\nabla U_a \frac{\partial \bar{f}_a^0}{\partial \mathbf{p}_a} \right] &= -\nabla U_a \frac{\beta}{\epsilon_a^0} \bar{f}_a^0(1 \pm \bar{f}_a^0) \\ &\quad + (\nabla U_a \cdot \mathbf{v}_a) \frac{\beta}{\epsilon_a^0} \bar{f}_a^0(1 \pm \bar{f}_a^0) \mathbf{v}_a \\ &\quad + (\nabla U_a \cdot \mathbf{v}_a) \beta^2 (1 \pm 2\bar{f}_a^0) \bar{f}_a^0(1 \pm \bar{f}_a^0) \mathbf{v}_a. \quad (63) \end{aligned}$$

Since Eqs. (60-63) involve a dot product with $\mathbf{v}_a \times \mathbf{H}$, certain vector components within these equations become irrelevant by the orthogonality condition $(\mathbf{v}_a \times \mathbf{H}) \cdot \mathbf{v}_a = 0$. Consequently, Eq. (56) can be simplified and rewritten as

$$\begin{aligned} 0 &= \frac{F_a}{\tau_a} \boldsymbol{\Xi} \cdot \mathbf{v}_a + \frac{Q_a}{\epsilon_a^0} F_a \mathbf{v}_a \times \mathbf{H} \cdot \boldsymbol{\Xi} + \frac{Q_a^2}{\epsilon_a^0} \tau_a F_a \mathbf{v}_a \times \mathbf{H} \cdot \mathbf{E} \\ &\quad + \frac{Q_a \tau_a}{\epsilon_a^0} \mathbf{v}_a \times \mathbf{H} \cdot \sum_q H_a^q \nabla \alpha_q. \quad (64) \end{aligned}$$

Through rigorous calculations, we obtain the following expression for $\boldsymbol{\Xi}$:

$$\begin{aligned} \boldsymbol{\Xi} &= \frac{\tau_a}{(\omega_{c,a}\tau_a)^2 + 1} \left[-\omega_{c,a}^2 Q_a \mathbf{E} + \frac{\omega_{c,a}}{\tau_a} Q_a (\mathbf{E} \times \mathbf{h}) \right. \\ &\quad \left. + \frac{\omega_{c,a} H_a^q}{\tau_a F_a} (\nabla \alpha_q \times \mathbf{h}) - \frac{\omega_{c,a}^2 H_a^q}{F_a} \nabla \alpha_q \right], \quad (65) \end{aligned}$$

where $\mathbf{h} = \mathbf{H}/H$. The magnetic field information is embedded in cyclotron frequency of particle species a , denoted by $\omega_{c,a} = Q_a H/\epsilon_a^0$. By inserting Eq. (65) into Eq. (55), we finally obtain the magnetic field-dependent

perturbation term of the distribution function,

$$\begin{aligned} \delta f_a &= \frac{\tau_a^2}{(\omega_{c,a}\tau_a)^2 + 1} \left[\omega_{c,a} F_a Q_a (\mathbf{E} \times \mathbf{h}) \cdot \mathbf{v}_a \right. \\ &\quad \left. + \frac{1}{\tau_a} F_a Q_a \mathbf{E} \cdot \mathbf{v}_a + \sum_q \omega_{c,a} H_a^q (\nabla \alpha_q \times \mathbf{h}) \cdot \mathbf{v}_a \right. \\ &\quad \left. + \sum_q \frac{1}{\tau_a} H_a^q \mathbf{v}_a \cdot \nabla \alpha_q \right]. \quad (66) \end{aligned}$$

Repeating some procedures in the previous subsection (Eqs. (17)-(30), Eqs. (36)-(45)), the particular solutions for the functions \mathcal{B}_a^q and \mathcal{G}_a from ϕ_a in the presence of a magnetic field are computed as

$$\begin{aligned} \mathcal{B}_{a,\text{part}}^{q,H \neq 0} &= \frac{\tau_a}{\epsilon_a^0} \left[q_a - \frac{n_q}{\omega} (\epsilon_a^0 + U_a) \right] (1 \pm \bar{f}_a^0) \\ &\quad \times \frac{[\omega_{c,a}\tau_a(\mathbf{h} \times \mathbf{v}_a) + 1]}{(\omega_{c,a}\tau_a)^2 + 1}, \quad (67) \end{aligned}$$

$$\mathcal{G}_{a,\text{part}}^{H \neq 0} = \frac{Q_a \tau_a}{\epsilon_a^0} (1 \pm \bar{f}_a^0) \frac{[1 + \omega_{c,a}\tau_a(\mathbf{h} \times \mathbf{v}_a)]}{(\omega_{c,a}\tau_a)^2 + 1}. \quad (68)$$

Upon substitution of Eq. (67) and Eq. (68) into Eq. (43), the diffusion current of the conserved charge q' in a magnetic field is given by:

$$\begin{aligned} \mathbf{V}^{q'} &= - \sum_{a,q} \int d\Gamma_a \frac{\mathbf{p}_a}{(\epsilon_a^0)^2} \frac{\tau_a \mathbf{p}_a \cdot [\omega_{c,a}\tau_a(\nabla \alpha_q \times \mathbf{h}) + \nabla \alpha_q]}{(\omega_{c,a}\tau_a)^2 + 1} \\ &\quad \times \left[q_a - (\epsilon_a^0 + U_a) \frac{n_q}{\omega} \right] \left[q'_a - (\epsilon_a^0 + U_a) \frac{n_{q'}}{\omega} \right] \\ &\quad \times \bar{f}_a^0(1 \pm \bar{f}_a^0) \\ &\quad + \sum_a q'_a \int d\Gamma_a \frac{\mathbf{p}_a}{(\epsilon_a^0)^2} \frac{Q_a \tau_a \mathbf{p}_a \cdot [\omega_{c,a}\tau_a(\mathbf{E} \times \mathbf{h}) + \mathbf{E}]}{(\omega_{c,a}\tau_a)^2 + 1} \\ &\quad \times \left[q'_a - \frac{n_{q'}}{\omega} (\epsilon_a^0 + U_a) \right] \bar{f}_a^0(1 \pm \bar{f}_a^0). \quad (69) \end{aligned}$$

Assuming the magnetic field is aligned with the z -axis, the above equation can be decomposed into x - and y -components, resulting in the following matrix form:

$$\begin{bmatrix} V_x^{q'} \\ V_y^{q'} \end{bmatrix} = \begin{bmatrix} \eta_{xx}^{Qq'Q} & \eta_{xy}^{Qq'Q} \\ \eta_{yx}^{Qq'Q} & \eta_{yy}^{Qq'Q} \end{bmatrix} \begin{bmatrix} E_x \\ E_y \end{bmatrix} + \sum_q \begin{bmatrix} \kappa_{xx}^{Qqq'} & \kappa_{xy}^{Qqq'} \\ \kappa_{yx}^{Qqq'} & \kappa_{yy}^{Qqq'} \end{bmatrix} \begin{bmatrix} -\nabla_x \alpha_q \\ -\nabla_y \alpha_q \end{bmatrix}. \quad (70)$$

Here, the thermoelectric conductivity tensors, denoted as $\eta^{Qq'Q}$, and diffusion coefficient tensors, denoted as $\kappa^{Qqq'}$, in a magnetic field satisfy the Onsager's reciprocity relation [75, 76]: $\kappa_{xx}^{Qqq'}(\eta_{xy}^{Qq'Q}) = \kappa_{yy}^{Qqq'}(\eta_{yx}^{Qq'Q})$ and $\kappa_{xy}^{Qqq'}(\eta_{xx}^{Qq'Q}) = -\kappa_{yx}^{Qqq'}(-\eta_{yy}^{Qq'Q})$. Accordingly, the magnetic field-dependent thermoelectric conductivity matrix element, $\eta_{xx}^{Qq'Q}$, and the Hall-like or transverse thermoelectric conductivity matrix element, $\eta_{yx}^{Qq'Q}$, can be expressed as

$$\begin{aligned} \begin{bmatrix} \eta_{xx}^{Qq'Q} \\ \eta_{yx}^{Qq'Q} \end{bmatrix} &= \sum_a \frac{d_a Q_a}{3T} \int \frac{d^3 p_a}{(2\pi)^3} \frac{\mathbf{p}_a^2}{(\epsilon_a^0)^2} \frac{(q'_a - (\epsilon_a^0 + U_a) \frac{n_{q'}}{\omega})}{(\omega_{c,a}\tau_a)^2 + 1} \\ &\quad \times \begin{bmatrix} \tau_a \\ -\omega_{c,a}\tau_a^2 \end{bmatrix} \bar{f}_a^0(1 \pm \bar{f}_a^0). \quad (71) \end{aligned}$$

Similarly, the magnetic field-dependent diffusion coefficient matrix element, $\kappa_{xx}^{Qqq'}$, and the Hall-like diffusion

coefficient matrix element, $\kappa_{yx}^{Qqq'}$, can be given as

$$\begin{aligned} \begin{bmatrix} \kappa_{xx}^{Qqq'} \\ \kappa_{yx}^{Qqq'} \end{bmatrix} &= \sum_a \frac{d_a}{3} \int \frac{d^3 p_a}{(2\pi)^3} \frac{\mathbf{p}_a^2}{(\epsilon_a^0)^2} \frac{(q_a - (\epsilon_a^0 + U_a) \frac{n_a}{\omega})}{(\omega_{c,a} \tau_a)^2 + 1} \\ &\times \left(q'_a - (\epsilon_a^0 + U_a) \frac{n_{q'}}{\omega} \right) \begin{bmatrix} \tau_a \\ -\omega_{c,a} \tau_a^2 \end{bmatrix} \\ &\times \bar{f}_a^0 (1 \pm \bar{f}_a^0). \end{aligned} \quad (72)$$

To better distinguish the expressions of transport coefficients under various transverse restriction conditions later, we convert Eq. (70) into the following matrix form:

$$\begin{bmatrix} E_x \\ E_y \\ V_x^{q''} \\ V_y^{q''} \end{bmatrix} = \begin{bmatrix} \rho_{xx}^{QQ} & \rho_{xy}^{QQ} & \sum_q -TM_{xx}^{QqQ} & \sum_q -TM_{xy}^{QqQ} \\ \rho_{yx}^{QQ} & \rho_{yy}^{QQ} & \sum_q -TM_{yx}^{QqQ} & \sum_q -TM_{yy}^{QqQ} \\ \Pi_{xx}^{Qq''Q} & \Pi_{xy}^{Qq''Q} & \sum_q \tilde{\kappa}_{xx}^{Qqq''} & \sum_q \tilde{\kappa}_{xy}^{Qqq''} \\ \Pi_{yx}^{Qq''Q} & \Pi_{yy}^{Qq''Q} & \sum_q \tilde{\kappa}_{yx}^{Qqq''} & \sum_q \tilde{\kappa}_{yy}^{Qqq''} \end{bmatrix} \begin{bmatrix} V_x^Q \\ V_y^Q \\ -\nabla_x \alpha_q \\ -\nabla_y \alpha_q \end{bmatrix}, \quad q \in \{B, Q, S\}, \quad q'' \in \{B, S\}. \quad (73)$$

Solving the set of coupled matrix equations (73) under the condition of vanishing gradients of transverse conserved charge chemical thermal potentials ($\nabla_y \alpha_q = 0$) with $\nabla_x \alpha_q = 0 = V_y^Q = 0$, then the electric resistance tensors, ρ^{QQ} ,s can be obtained as

$$\rho_{xx}^{QQ} = \rho_{yy}^{QQ} = \frac{E_x}{V_x^Q} \Big|_{\nabla_y \alpha_q = 0} = \frac{\eta_{xx}^{QQQ}}{(\eta_{xx}^{QQQ})^2 + (\eta_{xy}^{QQQ})^2}, \quad (74)$$

$$\rho_{yx}^{QQ} = -\rho_{xy}^{QQ} = \frac{E_y}{V_x^Q} \Big|_{\nabla_y \alpha_q = 0} = \frac{\eta_{xy}^{QQQ}}{(\eta_{xx}^{QQQ})^2 + (\eta_{xy}^{QQQ})^2}. \quad (75)$$

In a magnetic field, the Hall-like diffusion thermopower of conserved charge q , denoted as M_{yx}^{QqQ} , can emerge. Under the condition of $\nabla_y \alpha_q = 0$ with $V_x^Q = V_y^Q = 0$, the magnetic field-dependent diffusion thermopower and Hall-like diffusion thermopower of conserved charge q can be derived respectively as

$$M_{xx}^{QqQ} = \frac{E_x}{T \nabla_x \alpha_q} \Big|_{\nabla_y \alpha_q = 0} = \beta \rho_{xx}^{QQ} \kappa_{xx}^{QqQ} - \beta \rho_{xy}^{QQ} \kappa_{xy}^{QqQ}, \quad (76)$$

$$M_{yx}^{QqQ} = \frac{E_y}{T \nabla_x \alpha_q} \Big|_{\nabla_y \alpha_q = 0} = -\beta \rho_{xx}^{QQ} \kappa_{xy}^{QqQ} - \beta \rho_{xy}^{QQ} \kappa_{xx}^{QqQ}. \quad (77)$$

In the absence of a magnetic field, M_{xx}^{QqQ} simplifies to M^{Qq} . Utilizing the set of coupled equations (73), and subjecting to the condition of $\nabla_y \alpha_q = 0$ with $V_x^Q = V_y^Q = 0$, the magneto-thermoelectric modified diffusion coefficient, $\tilde{\kappa}_{xx}^{Qqq''}$, and Hall-like magneto-thermoelectric modified diffusion coefficient, $\tilde{\kappa}_{yx}^{Qqq''}$, can be computed

respectively as

$$\begin{aligned} \tilde{\kappa}_{xx}^{Qqq''} &= \frac{V_x^{q''}}{-\nabla_x \alpha_q} \Big|_{\nabla_y \alpha_q = 0} \\ &= \kappa_{xx}^{Qqq''} - \eta_{xx}^{Qq''Q} T M_{xx}^{QqQ} + \eta_{yx}^{Qq''Q} T M_{yx}^{QqQ}, \end{aligned} \quad (78)$$

$$\begin{aligned} \tilde{\kappa}_{yx}^{Qqq''} &= \frac{V_y^{q''}}{-\nabla_x \alpha_q} \Big|_{\nabla_y \alpha_q = 0} \\ &= \kappa_{yx}^{Qqq''} - \eta_{yx}^{Qq''Q} T M_{xx}^{QqQ} - \eta_{xx}^{Qq''Q} T M_{yx}^{QqQ}. \end{aligned} \quad (79)$$

In condensed matter physics, the Righi-Leduc effect or thermal Hall effect occurs when a transverse temperature gradient ($\nabla_y T$) is developed by a longitudinal temperature gradient ($\nabla_x T$) under a static magnetic field (H_z). The associated Righi-Leduc coefficient is determined under the transverse adiabatic condition, specifically when the transverse heat current (I_y) is zero. Similarly, in hadronic matter with multiple conserved charges, a transverse or Hall-like conserved charge density gradient ($\nabla_y \alpha_q$) perpendicular to both the $\nabla_x \alpha_q$ and H_z , can be induced. The corresponding coefficient is calculated under the condition of vanishing transverse diffusion current i.e., $V_y^{q''} = 0$. Therefore, utilizing the matrix Eq. (73), and enforcing the conditions $V_y^{q''} = V_x^Q = V_y^Q = 0$, the Righi-Leduc-type relation within the hadronic medium can be deduced as follows:

$$\begin{aligned} 0 &= \sum_q \tilde{\kappa}_{yx}^{Qqq''} \nabla_x \alpha_q + \sum_q \tilde{\kappa}_{xx}^{Qqq''} \nabla_y \alpha_q \\ \rightarrow \mathcal{L}_{V_y^{q''}=0}^q &= \frac{\nabla_y \alpha_q}{\nabla_x \alpha_q} \Big|_{V_y^{q''}=0} = \frac{\tilde{\kappa}_{xy}^{Qqq''}}{\tilde{\kappa}_{xx}^{Qqq''}}, \end{aligned} \quad (80)$$

where $\mathcal{L}_{V_y^{q''}=0}^q$ denotes Righi-Leduc-like coefficient. Accordingly, the magnetic field-dependent diffusion ther-

mopower under the condition of $V_y^{q''} = 0$ with $V_x^Q = V_y^Q = 0$ is computed as

$$M_{xx, V_y^{q''}=0}^{QqQ} = M_{xx}^{QqQ} - M_{yx}^{QqQ} \mathcal{L}_{V_y^{q''}=0}^q. \quad (81)$$

When the magnetic field is turned off, the expressions of transport coefficients become equivalent under various transverse condition: $\nabla_y \alpha_q = 0$ and $V_y^{q''} = 0$. Similarly, the magneto-thermoelectric modified diffusion coefficient under the condition of $V_y^{q''} = 0$ with $V_x^Q = V_y^Q = 0$, is computed as

$$\tilde{\kappa}_{xx, V_y^{q''}=0}^{Qqq''} = \tilde{\kappa}_{xx}^{Qqq''} - \tilde{\kappa}_{yx}^{Qqq''} \mathcal{L}_{V_y^{q''}=0}^q. \quad (82)$$

D. Thermal averaged relaxation time

Comparing Eq. (25) and Eq. (26), the mutual interaction information of all particle species is encoded in the relaxation time, τ_a . For the binary elastic collisions $a(p_a) + b(p_b') \rightarrow a(p_a'') + b(p_b''')$, the inverse of τ_a is given as

$$\tau_a^{-1} = \sum_b \gamma_{ab} \int d\Gamma'_b d\Gamma''_a d\Gamma'''_b W_{ab}(p_a, p_b' | p_a'', p_b''') \times \bar{f}_b^{0'} (1 \pm \bar{f}_a^{0''}) \frac{(1 \pm \bar{f}_b^{0''''})}{1 \pm \bar{f}_a^0}, \quad (83)$$

where the transition rate is given as

$$W_{ab} = \frac{(2\pi)^4 \delta^4(p_a + p_b' - p_a'' - p_b''')}{16\epsilon_a^0 \epsilon_b^0 \epsilon_a^{0''} \epsilon_b^{0'''}} |\bar{\mathcal{M}}_{ab \rightarrow ab}|^2. \quad (84)$$

Here, $|\bar{\mathcal{M}}|$ is the dimensionless transition amplitude averaged over the spin degeneracy factor in both initial and final states [77]. This is necessary to balance the degeneracy factors in the $d\Gamma_a$. To simplify the estimation of relaxation time, $(1 \pm \bar{f}_a^{0''}) \frac{(1 \pm \bar{f}_b^{0''''})}{1 \pm \bar{f}_a^0} \simeq 1$, and we utilize the formula of scattering cross section [78]

$$\sigma_{ab} = \frac{\int d\Gamma''_a d\Gamma'''_b (2\pi)^4 \delta^4(p_a + p_b' - p_a'' - p_b''') |\bar{\mathcal{M}}|^2}{16\epsilon_a^{0''} \epsilon_b^{0'''}} \frac{1}{\sqrt{(p_a \cdot p_b')^2 - m_a^2 m_b^2}}, \quad (85)$$

then we can rewrite τ_a^{-1} as

$$\tau_a^{-1} = \sum_b \gamma_{ab} \rho_b \sigma_{ab} v_{ab}, \quad (86)$$

where $\rho_b = \int d\Gamma'_b \bar{f}_b^{0'}$ is the number density of hadron species b . It is worth noting that the RMF interactions between hadrons can influence the scattering process by modifying the number density of hadron species b . Therefore, the number density of hadron species b needs to be distinguished in the IHRG model and the RMFHrg model. In Eq. (86), the relative velocity v_{ab} is defined as

$$v_{ab} = \frac{\sqrt{(\epsilon_a^0 \epsilon_b^{0'} - \mathbf{p}_a \cdot \mathbf{p}_b')^2 - m_a^2 m_b^2}}{\epsilon_a^0 \epsilon_b^{0'}}. \quad (87)$$

We shall consider the momentum-independent relaxation time, the thermal averaged cross section $\langle \sigma_{ab} v_{ab} \rangle$ can be given as

$$\langle \sigma_{ab} v_{ab} \rangle = \frac{\int d^3 p_a d^3 p_b' \bar{f}_a^0 \bar{f}_b^{0'} \sigma_{ab} v_{ab}}{\int d^3 p_a d^3 p_b' \bar{f}_a^0 \bar{f}_b^{0'}}. \quad (88)$$

In this study, all hadrons are regarded as hard spheres with the same radius r_h , and σ_{ab} is a constant given by $\sigma_{ab} = 4\pi r_h^2 = 30$ mb

IV. NUMERICAL RESULTS AND DISCUSSIONS

All calculations are performed in the condition of $n_S = 0 = \mu_Q = 0$ [41, 43], which is expected in the initial stages of heavy-ion collision [79, 80]. This specific condition gives rise to a nonzero strangeness chemical potential, which is a function of T and μ_B . In the HRG models, we include all hadrons listed in `Thermal-FIST` package, with a mass cutoff set at $\Lambda = 3.0$ GeV [81]. The BES program at RHIC covers beam energy from $\sqrt{s_{NN}} = 3$ GeV to 200 GeV, with the baryon chemical potential ranging from $\mu_B \simeq 0.75$ GeV to 0.02 GeV [82–84]. In this investigation, we focus on values of μ_B up to 0.6 GeV.

A. Results for vanishing magnetic field

To better understand the behaviors of the diffusion coefficient matrix later, we first thoroughly discuss the T and μ_B dependence of the scaled conductivity matrix $\sigma^{qq'}/T$, which is given as

$$\frac{\sigma^{qq'}}{T} = \sum_a \frac{d_a \beta^2}{3} \int \frac{d^3 p_a}{(2\pi)^3} \tau_a \frac{\mathbf{p}_a^2}{(\epsilon_a^0)^2} q_a' q_a \bar{f}_a^0 (1 \pm \bar{f}_a^0). \quad (89)$$

It is closely related to the diffusion coefficient matrix. At $\mu_B = 0$, $\sigma^{qq'}/T$ is equal to $\kappa^{qq'}/T^2$. The variation of $\sigma^{qq'}/T$ with respect to T and μ_B is determined by the interplay between charge number density (or distribution function) and scattering rate (or the relaxation time $\tau_a \sim 1/\Gamma_{\text{scatt}}$). In Fig. 1, we see that the magnitude of σ^{QQ}/T (σ^{QB}/T) for $\mu_B = 0$ decreases (increases) monotonically as T increases, on the other hand, both σ^{QS}/T and σ^{SS}/T first increase with T and then decrease, which are qualitatively consistent with the results from the SMASH simulation (symbol lines) [85]. The negative sign of σ^{SB}/T is attributed to the associated dominant carriers, i.e., hyperons carrying a positive baryon number with a negative strangeness. As shown in Fig. 1, all scaled conductivities obtained from the SMASH simulation using the Green-Kubo formalism are quantitatively larger than ours. We can also see that the effect of RMF interaction on the scaled conductivity matrix for $\mu_B = 0$ is minimal. This is because the RMF correction for $\mu_B = 0$ results in a small suppression of

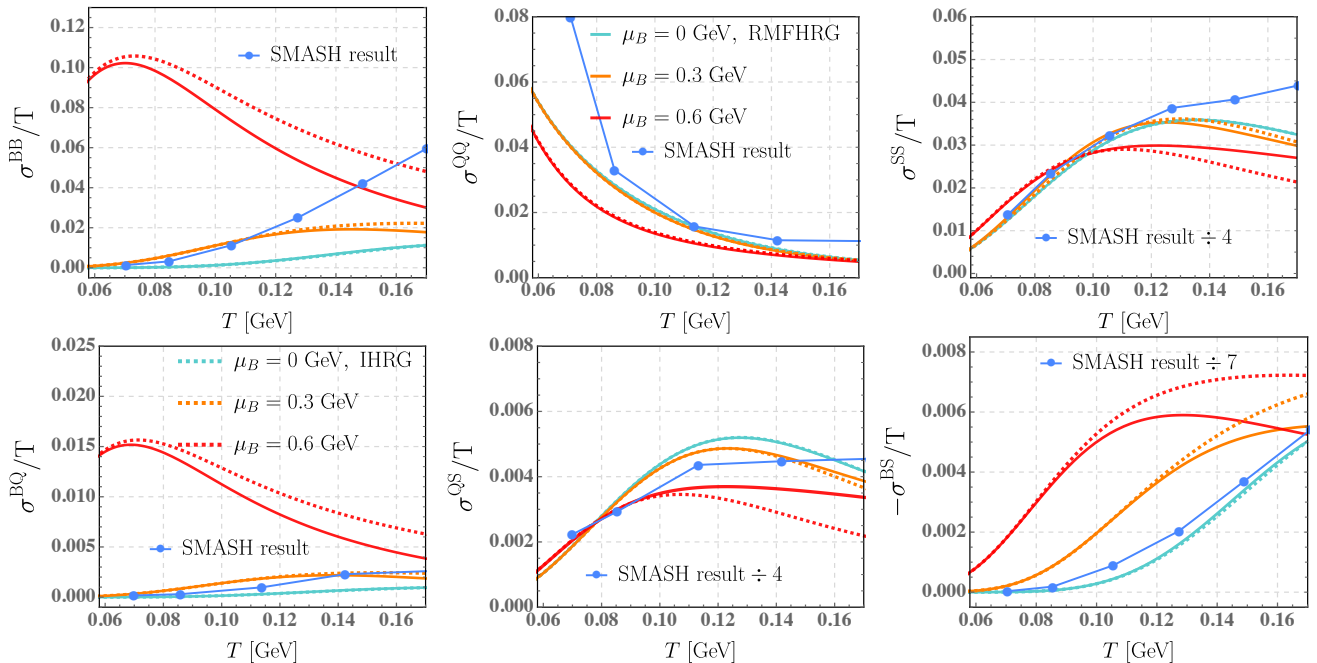


FIG. 1: The temperature dependence of complete scaled conductivity matrix $\sigma^{qq'}/T$ for different baryon chemical potentials, i.e., $\mu_B = 0$ (blue), 0.3 GeV (orange) and 0.6 GeV (red) in the IHRG model (dashed lines) and RMFHRG model (solid lines). The symbol lines are the estimations in the full SMASH simulation using the Green-Kubo formalism at zero μ_B [85].

charge number density and a slight enhancement of relaxation time, the mutual compensation makes the RMF correction on the conductivities negligible.

Compared to the thermal behaviors observed at $\mu_B = 0$ GeV, the scaled conductivities at $\mu_B = 0.3$ GeV remain largely unchanged. However, as illustrated in Fig. 1, there is a notable enhancement in the magnitude of σ^{qB}/T . This is because the dependence of σ^{qB}/T on μ_B is mainly governed by the baryon density, which is an increasing function of μ_B . Meanwhile, we observe a nominal reduction in both σ^{QS}/T and σ^{SS}/T when comparing their values at $\mu_B = 0.3$ GeV to those at $\mu_B = 0$ GeV. This reduction can be explained by the fact that the primary carriers for both σ^{QS}/T and σ^{SS}/T are kaons (K), the number density of kaons undergo a slight enhancement due to the nonzero μ_S , this enhancement is negated by the increased scattering rates of kaons resulting from their elevated collisions with baryons. The variation in σ^{QQ}/T at $\mu_B = 0.3$ GeV is invisible compared to that at $\mu_B = 0$ GeV. This minimal change is the result of a competition between meson (primarily pions) and baryon (primarily nucleons) contributions to σ^{QQ} . At $\mu_B = 0.3$ GeV, the decrease of pion contribution to σ^{QQ} with μ_B is nearly compensated by the increase of nucleon contribution to σ^{QQ} with μ_B . As μ_B increases further, the baryon density becomes more significant, resulting in pronounced changes in all conductivities at $\mu_B = 0.6$ GeV. We note that in comparison to the temperature dependence at $\mu_B = 0$ and 0.3 GeV, the

trend of both σ^{QB}/T and σ^{BB}/T at $\mu_B = 0.6$ GeV can undergo a reversal. This reversal arises because the decreasing behavior of the relaxation time for predominant nucleons with T dominates over the increasing trend of the distribution function with T . Compared to the variation in conductivity resulting from the RMF correction at lower μ_B ($\mu_B = 0$ or 0.3 GeV), all conductivities except σ^{QQ}/T , undergo notable changes when the RMF correction is considered at $\mu_B = 0.6$ GeV. In particular, σ^{BQ}/T , σ^{BB}/T , and $-\sigma^{BS}/T$ at $\mu_B = 0.6$ GeV show visible suppression due to the substantial reduction in baryon density of the system caused by the incorporation of the RMF correction. In contrast, the RMF correction significantly enhances σ^{QS}/T and σ^{SS}/T at $\mu_B = 0.6$ GeV. This enhancement is because the predominant carriers for both σ^{QS}/T and σ^{SS}/T at $\mu_B = 0.3$ GeV are still kaons, the RMF interaction between mesons affects the kaon density, while the relaxation time of kaons is influenced by the RMF interaction among various hadron-hadron pairs due to colliding with different hadrons. These effects seem to counteract each other at $\mu_B = 0.3$ GeV. However, as μ_B rises, the increase in kaon relaxation time caused by the RMF correction significantly overtakes the decrease in kaon density, leading to a substantial elevation in both conductivities at $\mu_B = 0.6$ GeV. For purely electric conductivity σ^{QQ}/T , it is nearly unaffected by the RMF correction even at high values of μ_B . The reason behind this is that the RMF correction on the meson and baryon contributions

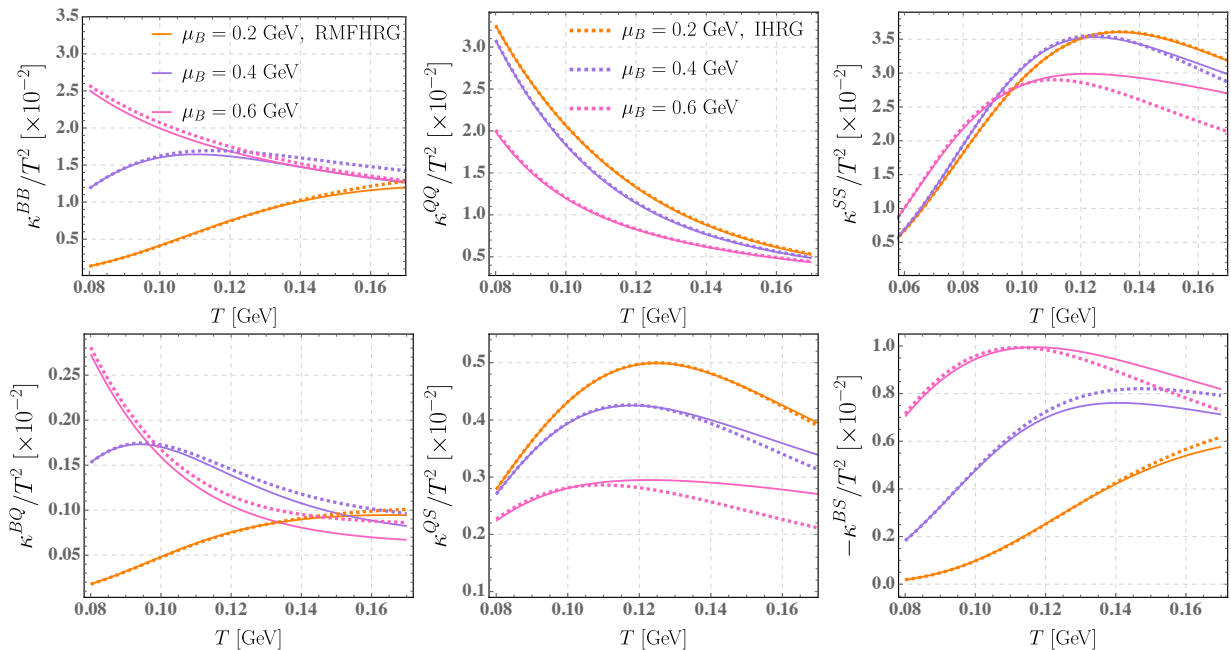


FIG. 2: The temperature dependence of scaled diffusion coefficient matrix $\kappa^{qq'}/T^2$ at $\mu_B = 0.2$ GeV (orange), 0.4 GeV (purple), 0.6 GeV (magenta) in the IHRG model (dashed lines) and RMFHRC model (solid lines).

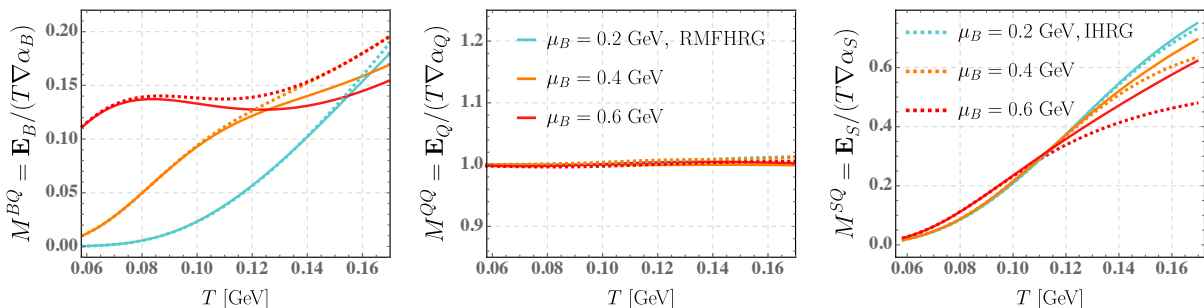


FIG. 3: The temperature dependence of conserved charge diffusion thermopower matrix M^{qQ} at $\mu_B = 0.2$ GeV (green), 0.4 GeV (orange), 0.6 GeV (red) in the IHRG model (dashed lines) and RMFHRC model (solid lines). The total induced electric field is presented as $\mathbf{E} = \mathbf{E}_B + \mathbf{E}_Q + \mathbf{E}_S$ with \mathbf{E}_q being the induced electric field by the gradient in conserved charge chemical potential μ_q .

to σ^{QQ}/T exactly cancel each other out. Overall, the μ_B and T dependence of all conductivities is unaltered by introducing RMF interactions.

Armed with the knowledge presented above, we can easily comprehend the results of the diffusion coefficient matrix. In Fig. 2, we display the T and μ_B dependence of the complete scaled diffusion coefficient matrix, $\kappa^{qq'}/T^2$, within both the IHRG and RMFHRC models. Akin to the conductivity matrix, the diffusion coefficient matrix elements $\kappa^{qq'}$ and $\kappa^{q'q}$ exhibit symmetry. The integrand of Eq. (47) decomposes the diffusion coefficient matrix element into $\sum_a [q_a q'_a + \tilde{\epsilon}_a^2 \frac{n_q n'_q}{\omega^2} + q'_a \tilde{\epsilon}_a \frac{n_q}{\omega} + q_a \tilde{\epsilon}_a \frac{n'_q}{\omega}] f_a^0 (1 \pm \tilde{f}_a^0)$. Within the considered T and μ_B region, the dominant values of $\tilde{\epsilon}_a$ in Eq. (47) are lower than ω/n_q . Conse-

quently, the qualitative behaviors of the scaled diffusion coefficient matrix are similar to the corresponding scaled conductivity matrix. From Fig. 2, we see that the off-diagonal elements can reach a magnitude comparable to the diagonal terms. Our results within the IHRG model align quantitatively and qualitatively with the results obtained by A. Das *et al.* [43] (for a more detailed analysis, see the Appendix). We note that the values of κ^{BB}/T^2 and κ^{QB}/T^2 for high T is larger at $\mu_B = 0.4$ GeV than at $\mu_B = 0.6$ GeV in the IHRG model. As the temperature rises sufficiently, κ^{QB}/T^2 at $\mu_B = 0.2$ GeV can even surpass that at $\mu_B = 0.4$ GeV. The decreasing dependence of κ^{BB} and κ^{QB} on μ_B in high T regions is consistent with the results in the QGP within dynamical quasi-particle

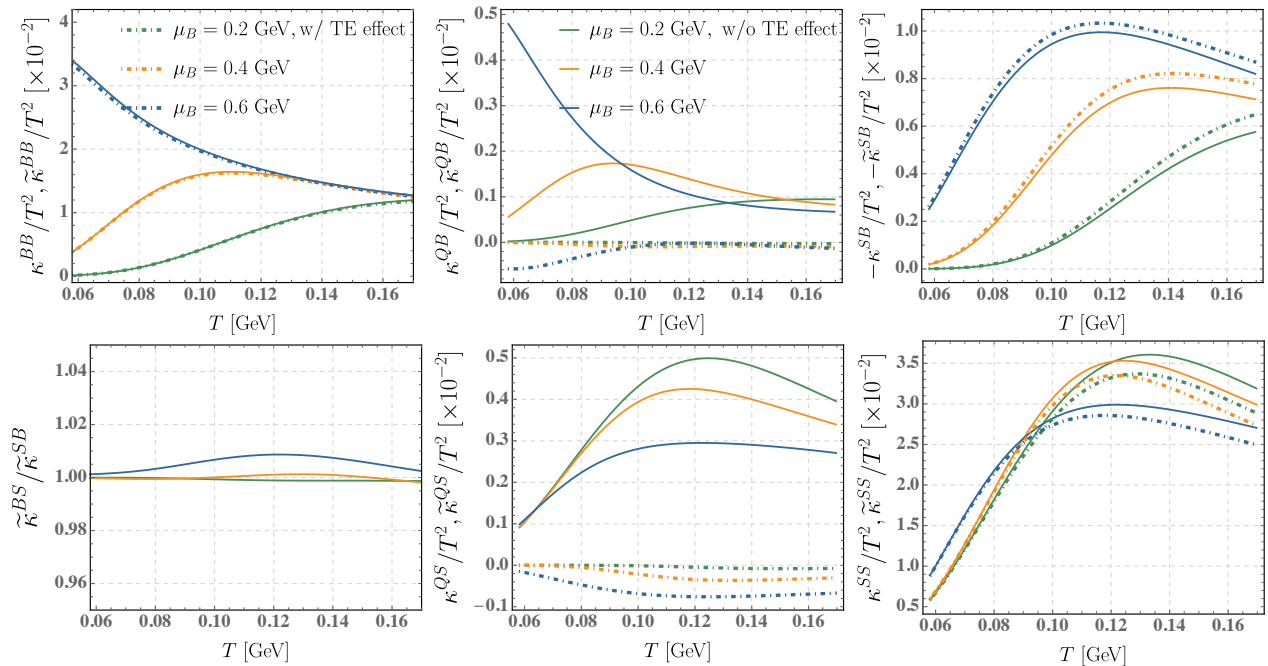


FIG. 4: The comparison between scaled diffusion coefficients matrix $\kappa^{qq'}/T^2$ (solid lines) and scaled thermoelectric modified diffusion coefficient matrix $\tilde{\kappa}^{qq'}/T^2$ (dot-dashed lines) in the RMFHRG model at $\mu_B = 0.2$ GeV (green), 0.4 GeV (orange), 0.6 GeV (blue). The below left panel represents the degree of asymmetry between $\tilde{\kappa}^{BS}$ and $\tilde{\kappa}^{SB}$.

model [42] and holographic model [86, 87]. Strikingly different from the σ^{BB}/T , the κ^{BB}/T^2 is nearly unaffected by the RMF interactions at $\mu_B = 0.6$ GeV, as depicted in Fig. 2. This phenomenon can be attributed to the near cancellation between the decrease in σ^{BB}/T and the increase in the integral of $\sum_a \tilde{\epsilon}_a^2 n_B^2 / (\omega^2 T^2) \tilde{f}_a^0 (1 \pm \tilde{f}_a^0)$ caused by the RMF correction in Eq. (47). In Fig. 2, it is also evident that the RMF correction can increase $-\kappa^{BS}/T^2$ at $\mu_B = 0.6$ GeV, which contrasts with the trend of $-\sigma^{BS}/T^2$ at $\mu_B = 0.6$ GeV, shown in Fig. 1. This can be well understood from Eq. (47), in which the integral term related to $-\sum_a S_a \tilde{\epsilon}_a n_B / (\omega T^2) \tilde{f}_a^0 (1 \pm \tilde{f}_a^0)$ is enhanced by the inclusion of RMF correction, and this enhancement can overwhelm the reduction in $-\sigma^{BS}$ caused by the RMF correction, thereby leading to an enhancement in $-\kappa^{BS}/T^2$. It is worth mentioning that, although in the statement of Refs. [40–42], the matching condition in the local rest frame is imposed during the derivation of diffusion coefficient matrix, the obtained formula bear similar to the $\eta^{qq'}T$ given in Eq. (48) excluding the quantum statistic effect and repulsive mean-field effect (for a detailed discussion, see the Appendix).

Until now, our analysis confines the scenario where the gradients of conserved charge densities are completely directly converted to diffusion currents. However, as mentioned in the introduction, these gradients can also generate an electric field, subsequently influencing the diffusion currents of conserved charges. To exhibit the response of the electric field to gradients in conserved charge chemical thermal potentials, we display the variations in the

diffusion thermopower matrix M^{qQ} with respect to T and μ_B within both the IHRG and RMFHRG models. As depicted in Fig. 3, both M^{BQ} and M^{SQ} are increasing functions with T , whereas the M^{QQ} remains almost unchanged and approaches 1. This behavior of M^{QQ} can well be understood from Eq. (50), wherein κ^{QQ}/T^2 is nearly equivalent in magnitude to η^{QQ}/T . Notably, M^{BQ} exhibits the smallest values, indicating a weak ability of the hadron gas (primarily protons) to convert the gradient of baryon chemical thermal potential into an electric field. With increasing μ_B , we observe a visible increase in M^{BQ} , while at high T , the values of M^{BQ} for different μ_B tend to converge. The decrease of M^{SQ} with respect to μ_B in high T regime is attributed that the strong dependence of κ^{SQ}/T^2 on μ_B dominates over the decreasing trend of T/η^{QQ} with respect to μ_B . Furthermore, as evident from Fig. 3, the RMF correction notably augments M^{SQ} and diminishes M^{BQ} at high μ_B . These responses primarily originate from κ^{SQ} and κ^{BQ} , respectively.

To intuitively illustrate the impact of the thermoelectric effect on the diffusion coefficient matrix, a comparison between $\kappa^{qq'}/T^2$ and $\tilde{\kappa}^{qq'}/T^2$ within the RMFHRG model is given in Fig. 4. When the thermoelectric effect is considered, diffusion coefficients in the electric current sector vanish, only those in the baryon and strangeness current sectors exist. Let's first explore the diffusion coefficients in the baryon current sector. From the upper panel of Fig. 4, it's evident that κ^{BB} is nearly unaffected by the thermoelectric effect. This observation can

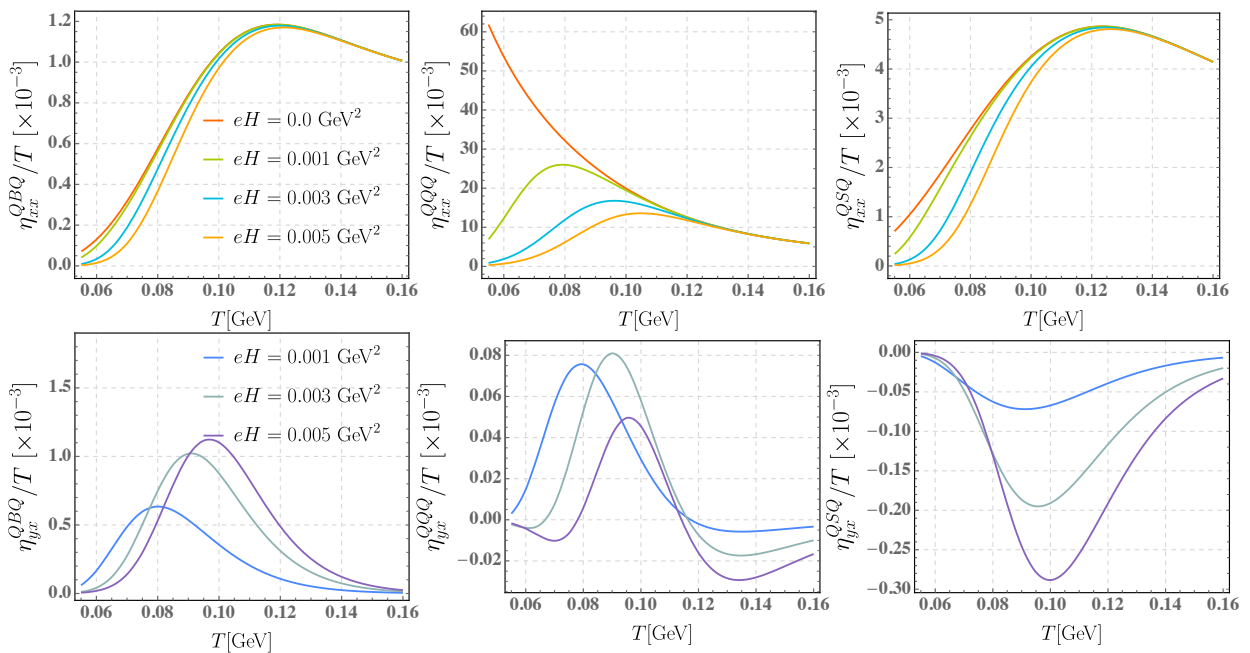


FIG. 5: Upper panel: the scaled magnetic field-dependent thermoelectric conductivity matrix η_{xx}^{QQ}/T as a function of temperature in the RMFHRG model for different values of the magnetic field, i.e., $eH = 0.0 \text{ GeV}^2$ (warm red), $eH = 0.001 \text{ GeV}^2$ (warm green), $eH = 0.003 \text{ GeV}^2$ (warm blue), $eH = 0.005 \text{ GeV}^2$ (warm orange) at $\mu_B = 0.3 \text{ GeV}$. Lower panel: the scaled Hall-like thermoelectric conductivity matrix η_{yx}^{QQ}/T as a function of temperature in the RMFHRG model for $eH = 0.001 \text{ GeV}^2$ (cool blue), $eH = 0.003 \text{ GeV}^2$ (cool green), $eH = 0.005 \text{ GeV}^2$ (cool purple) at $\mu_B = 0.3 \text{ GeV}$.

be well understood from Eq. (52), where the product of M^{BQ} and η^{BQ} is comparatively small compared to κ^{BB} . Different from κ^{BB}/T^2 , the inclusion of the thermoelectric effect obviously diminishes κ^{SS}/T^2 . Additionally, the thermoelectric effect enhances $-\kappa^{SB}/T^2$, which further reduces the net baryon current. Remarkably, the thermoelectric effect significantly suppresses κ^{QB}/T^2 (κ^{QS}/T^2), making $\tilde{\kappa}^{QB}$ ($\tilde{\kappa}^{QS}$) much smaller than κ^{BQ} (κ^{SQ}) and even altering its sign. These findings indicate that the thermoelectric effect significantly weakens the correlation between electric current and baryon (strangeness) current, rendering the gradient of electric chemical potential insignificant for baryon (strangeness) diffusion. As a consequence, the baryon diffusion current can be decreased by the thermoelectric effect, resulting in $V_B \approx \tilde{\kappa}^{BB}\nabla\alpha_B + \tilde{\kappa}^{BS}\nabla\alpha_S$ if gradients are of comparable magnitudes. As depicted in the lower left panel of Fig. 4, the inclusion of thermoelectric effect does not explicitly break the symmetry between $\tilde{\kappa}^{SB}$ and $\tilde{\kappa}^{BS}$. We remark that the T and μ_B dependence of $\tilde{\kappa}^{qq'}/T^2$ is still consistent with that of $\kappa^{qq'}/T^2$.

B. Results for finite magnetic field

We also study the magneto-thermoelectric effect of hadronic matter and examine its impact on both the

magnetic field-dependent diffusion coefficient matrix ($\kappa_{xx}^{Qqq'}$) and the Hall-like diffusion coefficient matrix ($\kappa_{yx}^{Qqq'}$). So far, the realistic time evolution of the initial magnetic field remains unclear. Based on the simple parametrization $eH(\sqrt{s_{NN}}) = 0.021\sqrt{s_{NN}}m_\pi^2$ (m_π is the pion mass) for Au+Au collisions with fixed collision parameter $b = 10 \text{ fm}$ [88], and using $eH = eH_0(\tau_0/\tau)^a$ with $a = 1$ as well as $eH \sim 4m_\pi^2$ for the thermalization timescale $\tau_0 \sim 1 \text{ fm}$, we estimate that for the hadronization time scale $\tau \sim 10 \text{ fm}$, eH would be approximately 0.008 GeV^2 . In our study, we consider a magnetic field region ranging from 0 to 0.005 GeV^2 , as done in Ref. [51].

All the estimations at finite magnetic fields are performed using the RMFHRG model, with a fixed baryon chemical potential $\mu_B = 0.3 \text{ GeV}$. As illustrated in the upper panel of Fig. 5, the temperature dependence of the scaled magnetic field-dependent thermoelectric conductivity, specifically $\eta_{xx}^{Qq'Q}/T$ where $q'' \in \{B, S\}$, remains unaltered at finite magnetic fields when compared to zero magnetic field. It is observed that η_{xx}^{QQ}/T at finite magnetic fields first increases with temperature and subsequently decreases. This non-monotonic behavior of η_{xx}^{QQ}/T with respect to T is primarily attributed to the combined effect of the magnetic field and relaxation time in the integrand of Eq. (71), which can be well understood in analogy with the discussion on magnetic field-dependent electric conductivity reported in previ-

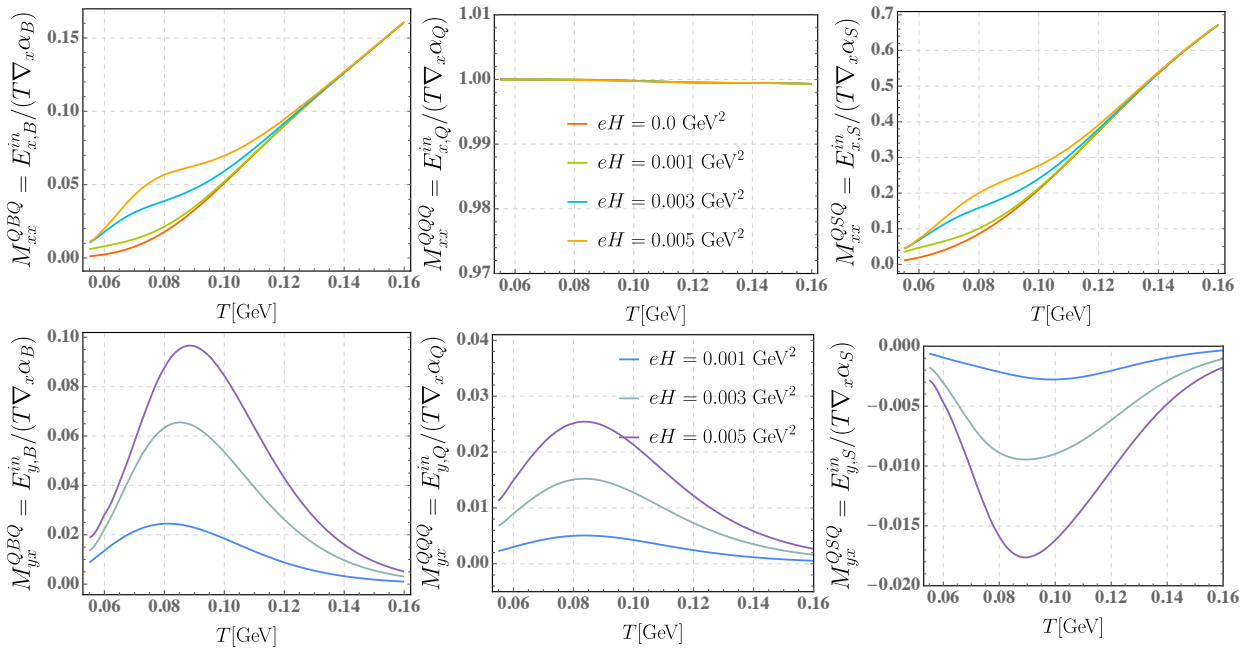


FIG. 6: Same as Fig. 5 but for magnetic field-dependent diffusion thermopower matrix M_{xx}^{QQQ} and Hall-like diffusion thermopower matrix M_{yx}^{QQQ} .

ous studies [44, 89, 90]. The dominant charge carriers for η_{yx}^{QQQ}/T are charged pions. At low T , the scattering rate of pions is smaller than cyclotron frequency (ω_c), resulting in $\frac{\tau_a}{(\omega_{c,a}\tau_a)^2+1} \sim 1/(\omega_{c,a}^2\tau_a)$. While, at high T , the pion scattering rate exceeds ω_c , leading to $\frac{\tau_a}{(\omega_{c,a}\tau_a)^2+1} \sim \tau_a$. Furthermore, all the scaled magnetic field-dependent thermoelectric conductivities initially decrease with increasing magnetic field before converging at high T . From the lower panel of Fig. 5, we also note that all scaled Hall-like thermoelectric conductivities, denoted as η_{yx}^{QQQ}/T , exhibit a non-monotonic temperature dependence. This behavior is attributed to the complex interplay of various factors, including relaxation time, cyclotron frequency, and the factor n_q/ω . In the hadron gas, the predominant contributions for η_{yx}^{QQQ}/T stem from protons (p) and Sigma baryons (Σ^+). We note that η_{yx}^{QSQ}/T takes on negative values. This can be understood through Eq. (71), where the dominant term in the integrand, $\sim \sum_a S_a Q_a \tilde{\epsilon}_a n_Q / \omega f_a^0 (1 + f_a^0)$, determine the sign of η_{yx}^{QSQ}/T . This sign is predominantly influenced by Sigma baryons. The dependence of η_{yx}^{QBQ}/T on the magnetic field is non-monotonic. This is because, the predominant proton scattering rate in low T region is much smaller than the corresponding $\omega_{c,a}$, resulting in $\frac{\omega_{c,a}\tau_a^2}{(\omega_{c,a}\tau_a)^2+1} \sim 1/\omega_{c,a}$. While in high T regions, the proton scattering rate plays a dominant role with $\omega_{c,a}\tau_a \ll 1$, leading to $\frac{\omega_{c,a}\tau_a^2}{(\omega_{c,a}\tau_a)^2+1} \sim \omega_{c,a}$. In contrast, the dependence of η_{yx}^{QSQ}/T on the magnetic field appears almost monotonic since the scattering rate of predominant Sigma baryons is always larger than $\omega_{c,a}$ in

the entire T region considered. Additionally, we note the magnetic field dependence of η_{yx}^{QQQ}/T is akin to that of η_{yx}^{QBQ}/T , but its sign differs at low and high T . This variance is attributed to the shifting predominant contribution from protons at lower T and Sigma baryons at higher T .

Next, we discuss the qualitative behaviors of both magnetic field-dependent diffusion thermopower matrix, M_{xx}^{QQQ} , and Hall-like diffusion thermopower matrix, M_{yx}^{QQQ} , with respect to temperature and magnetic field, respectively. As shown in the upper panel of Fig. 6, the application of a magnetic field enhances both M_{xx}^{QBQ} and M_{xx}^{QSQ} in low T region, which means the ability of the hadron gas to convert baryon and strangeness chemical potential gradients into an electric field is strengthened by adding a magnetic field. Whereas the M_{xx}^{QQQ} appears to be independent of the magnetic field. All components of M_{yx}^{QQQ} exhibit a significant dependence on the magnetic field in the studied temperature region. As seen in the lower panel of Fig. 6, all M_{yx}^{QQQ} components in magnitude display a similar peak structure throughout the entire T region, and these magnitudes increase as eH increases. It's worth noting that the magnitude of M_{yx}^{QBQ} is comparable to that of M_{xx}^{QBQ} at low T .

As in the case without a magnetic field, we also compare the magnetic field-dependent diffusion coefficient matrix before and after accounting for the magneto-thermoelectric effect. As illustrated in Fig. 7, we note that all components of κ_{xx}^{QQQ}/T^2 , except for κ_{xx}^{QQQ}/T^2 , remain qualitatively unchanged in the presence of a magnetic field. The associated explanation of κ_{xx}^{QQQ}/T^2 mir-

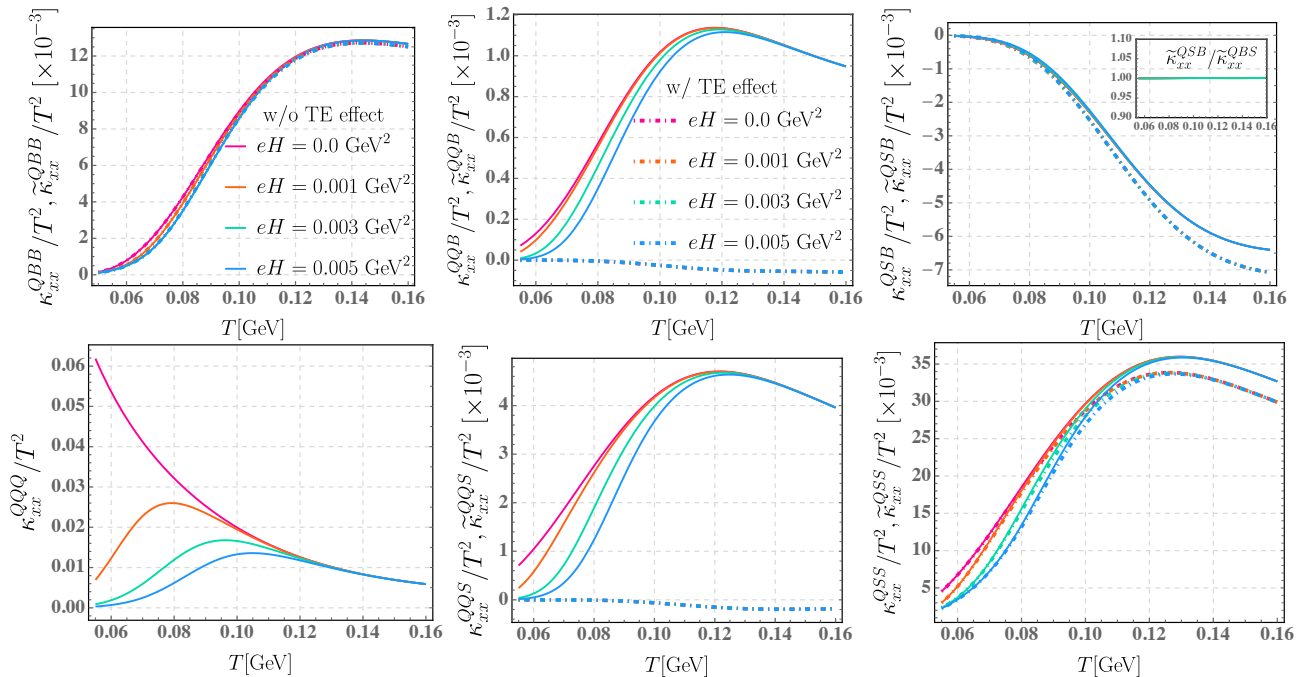


FIG. 7: Both complete scaled magnetic field-dependent diffusion coefficient matrix $\kappa_{xx}^{Qq'}/T^2$ (solid lines) and complete scaled magneto-thermoelectric modified diffusion coefficient matrix $\tilde{\kappa}_{xx}^{Qq''}/T^2$ (dot-dashed lines) for $eH = 0.0 \text{ GeV}^2$ (magenta), 0.001 GeV^2 (red), 0.003 GeV^2 (green), 0.005 GeV^2 (blue) at $\mu_B = 0.3 \text{ GeV}$ in the RMFHRG model. The inset in the upper right panel quantifies the degree of asymmetry between $\tilde{\kappa}_{xx}^{QBS}$ and $\tilde{\kappa}_{xx}^{QSB}$.

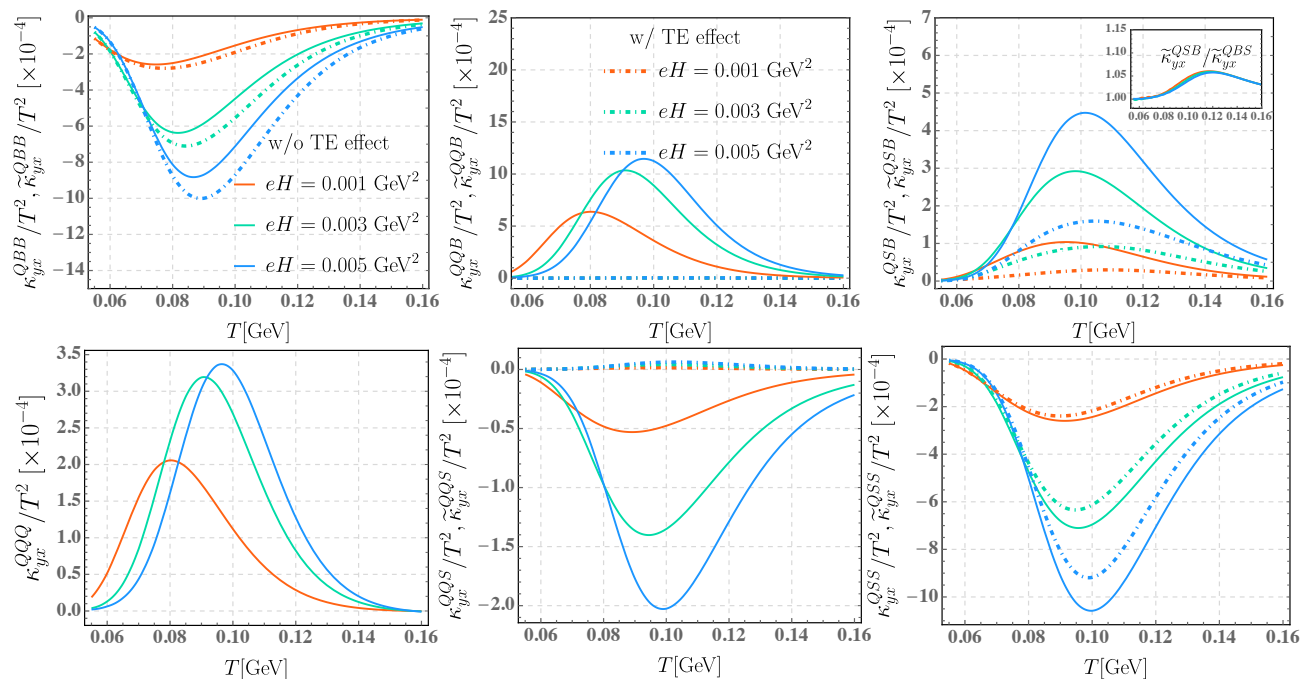


FIG. 8: Same as Fig. 7 for both complete scaled Hall-like diffusion coefficient matrix $\kappa_{yx}^{Qq'}/T^2$ and complete scaled magneto-thermoelectric modified Hall-like diffusion coefficient matrix $\tilde{\kappa}_{yx}^{Qq''}/T^2$.

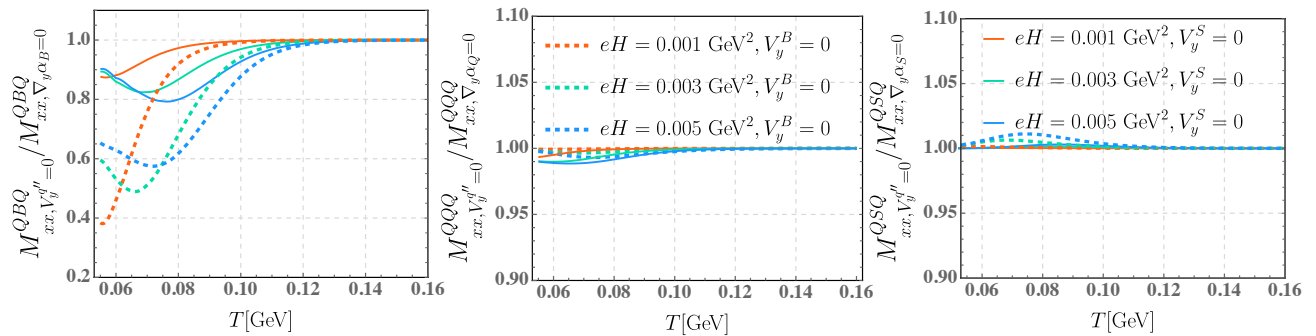


FIG. 9: The ratio of magnetic field-dependent diffusion thermopower under the condition of $V_y^{q''} = 0$ to that under the condition of $\nabla_y \alpha_q = 0$ as a function of temperature at $eH = 0.001 \text{ GeV}^2$ (red), 0.003 GeV^2 (green), 0.005 GeV^2 (blue). The dashed lines and solid lines correspond to the results under the condition of $V_y^B = 0$ and the condition of $V_y^S = 0$, respectively. All the numerical calculations are performed at $\mu_B = 0.3 \text{ GeV}$ in the RMFHRG model.

rors that of η_{xx}^{QQQ}/T . Within the baryon current sector, κ_{xx}^{QBB} and κ_{xx}^{QSB} appear insensitive to the magnetic field, while the remaining terms exhibit significant reductions in the low T region when the magnetic field is introduced. Thus, the presence of a magnetic field can significantly hinder the strangeness and electric diffusion, especially when gradients of similar magnitudes are involved. The qualitative behavior of the magneto-thermoelectric modified diffusion coefficient matrix, $\tilde{\kappa}_{xx}^{Qqq''}$, aligns with that of the non-modified matrix, $\kappa_{xx}^{Qqq''}$. Furthermore, as depicted in the inset of the upper right panel of Fig. 7, the symmetry between $\tilde{\kappa}_{xx}^{QSB}$ and $\tilde{\kappa}_{xx}^{QBS}$ is almost maintained.

In comparison to $\kappa_{xx}^{Qqq'}/T^2$, all Hall-like diffusion coefficient matrix elements, $\kappa_{yx}^{Qqq'}/T^2$, exhibit a strong dependence on the magnetic field, as shown in Fig. 8, and display a peak structure in magnitude. The explanation for the behavior of $\kappa_{yx}^{Qqq'}/T^2$ with respect to T and eH is akin to that of $\eta_{yx}^{Qqq'}/T^2$. It's worth noting that $\kappa_{yx}^{Qqq''}/T^2$ show obvious responses to the magneto-thermoelectric effect. The magneto-thermoelectric effect can considerably diminish the magnitude of $\tilde{\kappa}_{yx}^{QQB}$ ($\tilde{\kappa}_{yx}^{QQS}$), thereby rendering the transverse coupling between electric charge and baryon (strangeness) charge insignificant in Hall-like baryon (strangeness) current. Strikingly different from κ_{xx}^{QBB} , we observe that the magneto-thermoelectric effect gives an obvious enhancement in the magnitude of κ_{yx}^{QBB} . The eH and T dependence of $\tilde{\kappa}_{yx}^{Qqq''}$ remains similar to that of $\kappa_{yx}^{Qqq''}$. Notably, the introduction of the magneto-thermoelectric effect causes a significant asymmetry between $\tilde{\kappa}_{yx}^{QSB}$ and $\tilde{\kappa}_{yx}^{QBS}$, as depicted in the inset of the upper right panel of Fig. 8. This asymmetry intensifies further with the increase in μ_B .

The aforementioned calculations regarding magnetic field-dependent diffusion thermopower matrix and magneto-thermoelectric modified diffusion coefficient matrix in the presence of a magnetic field were performed under the assumption that the conserved charge chemical thermal potential gradients are solely along the longitudi-

nal direction, specifically with, $\nabla_x \alpha_q \neq 0$, $\nabla_y \alpha_q = 0$. As stated in Sec. III, under the condition of zero transverse diffusion current of conserved charge, (i.e., $V_y^{q''} = 0$ with $q'' \in \{B, S\}$), a transverse gradient $\nabla_y \alpha_q$ can arise from $\nabla_x \alpha_q$, subsequently inducing a transverse electric field. Under these conditions, the magnitude of the magneto-thermoelectric modified diffusion coefficient matrix might differ from that under the condition of $\nabla_y \alpha_q = 0$. To intuitively quantify the impact of varying transverse conditions, Fig. 9 illustrate the ratio of magnetic field-dependent diffusion thermopower computed under the conditions of $V_y^B = 0$ and $V_y^S = 0$ to that determined under the condition of $\nabla_y \alpha_q = 0$. We find that imposing the condition of $V_y^{q''} = 0$ results in an obvious reduction in M_{xx}^{QBQ} within low T region, whereas both M_{xx}^{QQQ} and M_{xx}^{QSQ} exhibit almost insensitive to alterations in transverse conditions. This result is unsurprising since, under the condition of $\nabla_y \alpha_q = 0$, the values of M_{yx}^{QQQ} (M_{yx}^{QSQ}) is much smaller than the corresponding M_{xx}^{QQQ} (M_{xx}^{QSQ}), as shown in Fig. 6. Additionally, the $\mathcal{L}_{V_y^{q''}=0}^q$ always remains less than 1 due to $|\tilde{\kappa}_{yx}^{Qqq''}| < |\tilde{\kappa}_{xx}^{Qqq''}|$, consequently, the product of M_{yx}^{QQQ} (M_{yx}^{QSQ}) and $\mathcal{L}_{V_y^{q''}=0}^q$ in Eq. (81) is negligible in comparison to M_{xx}^{QQQ} (M_{xx}^{QSQ}).

Finally, we show the sensitivity of magneto-thermoelectric modified diffusion coefficient matrix, $\tilde{\kappa}_{xx}^{Qqq''}$, to various choices of transverse conditions in Fig. 10. The results for $\tilde{\kappa}_{xx}^{QQB}$ and $\tilde{\kappa}_{xx}^{QQS}$ are not presented here as they are much smaller than the other terms. We observe that taking the condition of $\nabla_y \alpha_q = 0$ as a baseline, the variation of $\tilde{\kappa}_{xx}^{Qqq''}$ due to changes in transverse conditions is generally small, except that $\tilde{\kappa}_{xx}^{QBB}$ has a slight reduction in the condition of $V_y^B = 0$ at low T . The qualitative features of $\tilde{\kappa}_{xx}^{Qqq''}$ almost remain unchanged under various transverse conditions.

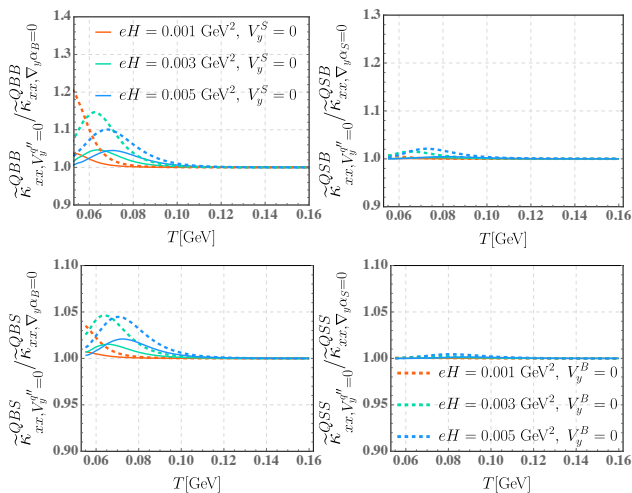


FIG. 10: Same as Fig. 9 but for the ratio of magneto-thermoelectric modified diffusion coefficient under the condition of $V_y^{q''} = 0$ to that under the condition of $\nabla_y \alpha_q = 0$.

V. SUMMARY

We investigated the thermoelectric effect and diffusion process involving multiple conserved charges in hot and dense hadronic matter. Their corresponding diffusion thermopower matrix M^{qQ} and diffusion coefficient matrix $\kappa^{qq'}$ with $q, q' \in \{B, Q, S\}$ were evaluated in both the IHRG and RMFHRG models by solving the relativistic Boltzmann equation under relaxation time approximation, where the Landau-Lifshitz energy frame was adopted. In the RMFHRG model, the repulsive interaction between hadrons is treated as a density-dependent mean-field potential, leading to a shift in the single-particle energy. In the presence of a magnetic field, additional Hall-like diffusion thermopower matrix M_{yx}^{QQQ} and Hall-like diffusion coefficient matrix $\kappa_{yx}^{QQq'}$ emerge. We further explored the impact of the magneto-thermoelectric effect on both $\kappa_{xx}^{QQq'}$ and $\kappa_{yx}^{QQq'}$. Additionally, we studied the sensitivities of magnetic field-dependent diffusion thermopower matrix M_{xx}^{QQQ} and magneto-thermoelectric modified diffusion coefficient matrix $\tilde{\kappa}_{xx}^{QQq''}$ (where $q'' \in \{B, S\}$) to various transverse restrictions. Below, we outline the primary findings emerging from our research.

- All the scaled diffusion coefficients, except for κ^{QQ}/T^2 and κ^{BB}/T^2 are sensitive to the RMF interactions in the baryon-rich region, indicating that the repulsive interactions between hadrons are crucial for understanding the diffusion properties of QCD matter created at the lower collision energies.
- Both M^{BQ} and M^{SQ} exhibit a strong dependence on T and μ_B . In contrast, the M^{QQ} remains almost unaffected by varying T and μ_B , maintaining

a value close to 1. The introduction of RMF corrections leads to a substantial increase in M^{SQ} and a decrease in M^{BQ} at large μ_B .

- The thermoelectric effect generally hinders baryon (strangeness) diffusion and significantly weakens the correlation between electric charge and baryon number (strangeness).
- In the magnetic field, both M_{xx}^{QBB} and M_{xx}^{QSQ} increase with the magnetic field at low T , whereas M_{xx}^{QQQ} is almost magnetic field independent. The magnitude of the Hall-like diffusion thermopower matrix is considerably influenced by eH and exhibits a distinct peak structure in the considered T region. Compared to M_{xx}^{QQQ} and M_{xx}^{QSQ} , the magnitude of M_{xx}^{QBB} at low T is more sensitive to variations in transverse restriction conditions.
- Apart from κ_{xx}^{QBB} and κ_{xx}^{QSB} , the other diffusion coefficients are sensitive to eH and decrease with eH at low T , indicating that the magnetic field can impede the electric charge and strangeness diffusion. Furthermore, the quantitative and qualitative characteristics of $\tilde{\kappa}_{xx}^{QQq''}$ remain relatively stable under varying transverse restriction conditions.
- The full Hall-like diffusion coefficients in magnitude reveal a similar peak structure in the considered T region and exhibit a strong dependence on the magnetic field. Notably, the inclusion of the magneto-thermoelectric effect can result in asymmetry between $\tilde{\kappa}_{yx}^{QSB}$ and $\tilde{\kappa}_{yx}^{QBS}$.

These findings could offer valuable insights into the dynamics of various conserved charges and contribute to the development of dissipative (magneto-)hydrodynamics frameworks that explicitly incorporate multiple conserved charges.

ACKNOWLEDGMENTS

This work was supported by Guangdong Major Project of Basic and Applied Basic Research No. 2020B0301030008 and No. 2022A1515010683, the Natural Science Foundation of China No.12247132, and the China Postdoctoral Science Foundation No.2023M731159.

APPENDIX

In Fig. 11, we present a comparison between the diffusion coefficient matrix result obtained in this study and the one reported by A. Das *et al.* in Ref. [43] within the framework of the IHRG model. The diffusion coefficient

matrix $\kappa^{qq'}$ derived in Ref. [43] takes the following form:

$$\kappa^{qq'} = \sum_a \frac{d_a}{3} \int \frac{d^3 p_a}{(2\pi)^3} \tau_a \frac{\mathbf{p}_a^2}{(\epsilon_a^0)^2} \left[q'_a - \epsilon_a^0 \frac{n'_q}{\omega} \right] \times \left[q_a - \epsilon_a^0 \frac{n_q}{\omega} \right] f_a^{(0)}, \quad (90)$$

where $f_a^{(0)}$ represents the equilibrium distribution function in the classical limit, i.e., the Boltzmann distribution function. As illustrated in Fig. 11, our results for the full diffusion coefficient align closely with those reported by A. Das *et al.* The numerical discrepancies primarily arise from the choices in degrees of freedom and the absence of quantum statistic effect in [43].

Alternatively, we note that the expression of $\kappa^{qq'}$ presented in Refs [40–42] differs from ours. In those references, $\kappa^{qq'}$ is expressed as

$$\kappa^{qq'} = \frac{\tau}{3} \sum_a \frac{d^3 p_a}{(2\pi)^3} \frac{\mathbf{p}_a^2}{(\epsilon_a^0)^2} \left(q'_a - \frac{\epsilon_a^0 n'_q}{\omega} \right) q_a f_a^{(0)}. \quad (91)$$

In Ref. [41], a constant relaxation time τ for all the hadron species is employed. Comparing with our thermoelectric transport coefficient $\eta^{qq'}$ from Eq. (48), we find that $\eta^{qq'}/T$ bears formal resemblance to $\kappa^{qq'}/T^2$ derived in Refs. [40–42], discounting the quantum statistic effect and repulsive mean-field effect. As shown in Fig. 12, our results are smaller than those reported in Ref. [41], and the qualitative behaviors of $\eta^{qq'}/T^2$ in the baryon diffusion current are also slightly different from the results in Ref. [41]. It is clear that η^{BS}/T in Fig. 12 is not equivalent to η^{SB}/T at $\mu_B = 0.6$ GeV. This indicates that the symmetry of the off-diagonal diffusion coefficients ($\kappa^{qq'} = \kappa^{q'q}$) reported in Refs. [40, 41] may not hold true when the quantum statistic effects are considered. By comparing Fig. 2 and Fig. 12, we observe that the quantitative and qualitative differences between $\kappa^{qq'}/T^2$ and $\eta^{qq'}/T$ are negligible. Therefore, the numerical discrepancy between our diffusion coefficient matrix and that of Ref. [41] can primarily be attributed to differences in the degrees of freedom and relaxation times.

-
- [1] I. Arsene *et al.* [BRAHMS], Nucl. Phys. A **757**, 1-27 (2005)
- [2] B. B. Back *et al.* [PHOBOS], Nucl. Phys. A **757**, 28-101 (2005).
- [3] K. Adcox *et al.* [PHENIX], Nucl. Phys. A **757**, 184-283 (2005).
- [4] J. Adams *et al.* [STAR], Nucl. Phys. A **757**, 102-183 (2005).
- [5] K. Aamodt *et al.* [ALICE], Phys. Rev. Lett. **105**, 252301 (2010).
- [6] S. Chatrchyan *et al.* [CMS], JHEP **08**, 141 (2011).
- [7] G. Aad *et al.* [ATLAS], Phys. Lett. B **707**, 330-348 (2012).
- [8] S. Chatrchyan *et al.* [CMS], Eur. Phys. J. C **72**, 2012 (2012).
- [9] S. Chatrchyan *et al.* [CMS], Phys. Rev. C **84**, 024906 (2011).
- [10] K. Aamodt *et al.* [ALICE], Phys. Lett. B **696**, 30-39 (2011).
- [11] Y. Aoki, G. Endrodi, Z. Fodor, S. D. Katz and K. K. Szabo, Nature **443**, 675-678 (2006).
- [12] M. Cheng, N. H. Christ, S. Datta, J. van der Heide, C. Jung, F. Karsch, O. Kaczmarek, E. Laermann, R. D. Mawhinney and C. Miao, *et al.* Phys. Rev. D **74**, 054507 (2006).
- [13] O. Philipsen, Prog. Part. Nucl. Phys. **70**, 55-107 (2013).
- [14] Y. Nambu and G. Jona-Lasinio, Phys. Rev. **122**, 345-358 (1961).
- [15] T. Hatsuda and T. Kunihiro, Phys. Rept. **247**, 221-367 (1994).
- [16] K. Fukushima, Phys. Rev. D **77**, 114028 (2008) [erratum: Phys. Rev. D **78**, 039902 (2008)].
- [17] B. J. Schaefer and J. Wambach, Phys. Rev. D **75**, 085015 (2007).
- [18] B. J. Schaefer and M. Wagner, Phys. Rev. D **79**, 014018 (2009).
- [19] B. J. Schaefer, J. M. Pawłowski and J. Wambach, Phys. Rev. D **76**, 074023 (2007).
- [20] B. J. Schaefer and M. Wagner, Phys. Rev. D **85**, 034027 (2012).
- [21] R. A. Lacey, Phys. Rev. Lett. **114**, no.14, 142301 (2015).
- [22] M. M. Aggarwal *et al.* [STAR], [arXiv:1007.2613 [nucl-ex]].
- [23] B. Mohanty [STAR], J. Phys. G **38**, 124023 (2011).
- [24] N. A. Tahir, C. Deutsch, V. E. Fortov, V. Gryaznov, D. H. H. Hoffmann, M. Kulish, I. V. Lomonosov, V. Mintsev, P. Ni and D. Nikolaev, *et al.* Phys. Rev. Lett. **95**, 035001 (2005).
- [25] T. Ablyazimov *et al.* [CBM], Eur. Phys. J. A **53**, no.3, 60 (2017).
- [26] B. Friman, C. Hohne, J. Knoll, S. Leupold, J. Randrup, R. Rapp, and P. Senger, *The CBM Physics Book: Compressed Baryonic Matter in Laboratory Experiments* (Springer, New York, 2011).
- [27] V. Kekelidze, R. Lednicky, V. Matveev, I. Meshkov, A. Sorin and G. Trubnikov, Phys. Part. Nucl. Lett. **9**, 313-316 (2012).
- [28] P. Romatschke and U. Romatschke, Phys. Rev. Lett. **99**, 172301 (2007).
- [29] P. Kovtun, D. T. Son and A. O. Starinets, Phys. Rev. Lett. **94**, 111601 (2005).
- [30] U. Heinz and R. Snellings, Ann. Rev. Nucl. Part. Sci. **63**, 123-151 (2013).
- [31] N. Demir and S. A. Bass, Phys. Rev. Lett. **102**, 172302 (2009).
- [32] C. Sasaki and K. Redlich, Phys. Rev. C **79**, 055207 (2009).
- [33] F. Karsch, D. Kharzeev and K. Tuchin, Phys. Lett. B **663**, 217-221 (2008).
- [34] H. B. Meyer, Phys. Rev. Lett. **100**, 162001 (2008).
- [35] V. Voronyuk, V. D. Toneev, W. Cassing, E. L. Bratkovskaya, V. P. Konchakovski and

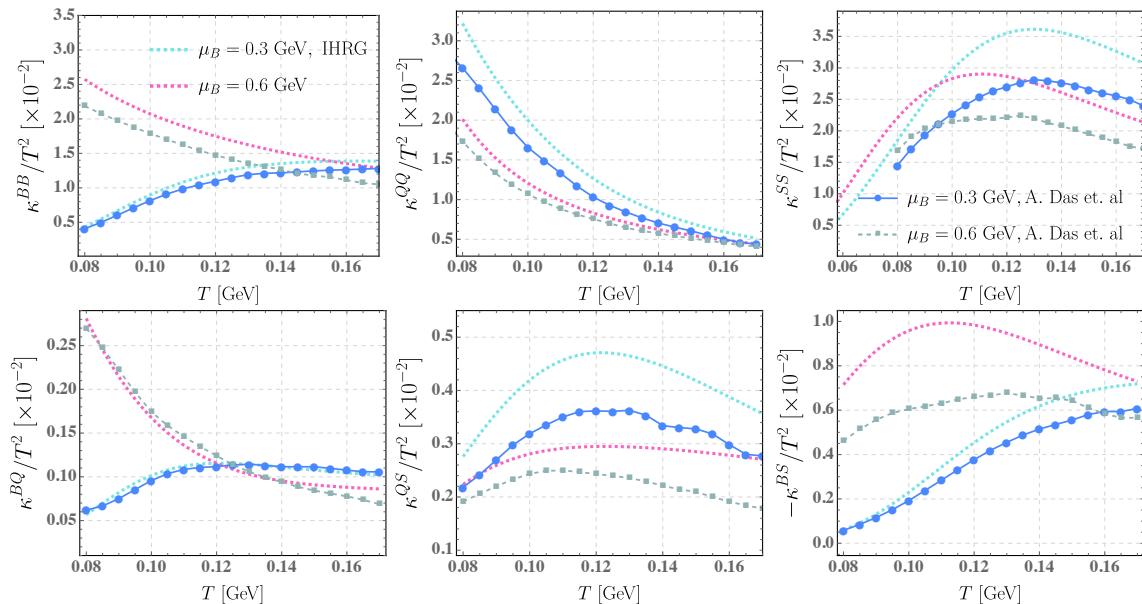


FIG. 11: The diffusion coefficient matrix results obtained by A. Das *et al.* (symbol lines) [43] is compared to our results (dashed lines) in the IHRG model with the same settings ($n_S = 0$, $\mu_Q = 0$) at $\mu_B = 0.3$ GeV and $\mu_B = 0.6$ GeV.

- S. A. Voloshin, Phys. Rev. C **83**, 054911 (2011).
- [36] K. Tuchin, Phys. Rev. C **83**, 017901 (2011).
- [37] L. McLerran and V. Skokov, Nucl. Phys. A **929**, 184-190 (2014).
- [38] V. Roy, S. Pu, L. Rezzolla and D. Rischke, Phys. Lett. B **750**, 45-52 (2015).
- [39] V. Roy, S. Pu, L. Rezzolla and D. H. Rischke, Phys. Rev. C **96**, no.5, 054909 (2017).
- [40] M. Greif, J. A. Fotakis, G. S. Denicol and C. Greiner, Phys. Rev. Lett. **120**, no.24, 242301 (2018).
- [41] J. A. Fotakis, M. Greif, C. Greiner, G. S. Denicol and H. Niemi, Phys. Rev. D **101**, no.7, 076007 (2020).
- [42] J. A. Fotakis, O. Soloveva, C. Greiner, O. Kaczmarek and E. Bratkovskaya, Phys. Rev. D **104**, no.3, 034014 (2021).
- [43] A. Das, H. Mishra and R. K. Mohapatra, Phys. Rev. D **106**, no.1, 014013 (2022).
- [44] H. X. Zhang, J. W. Kang and B. W. Zhang, Eur. Phys. J. C **81**, no.7, 623 (2021).
- [45] A. Das and H. Mishra, Eur. Phys. J. ST **230**, no.3, 607-634 (2021).
- [46] H. X. Zhang, Y. X. Xiao, J. W. Kang and B. W. Zhang, Nucl. Sci. Tech. **33**, no.11, 150 (2022).
- [47] M. Kurian, Phys. Rev. D **103**, no.5, 054024 (2021).
- [48] D. Dey and B. K. Patra, Phys. Rev. D **102**, no.9, 096011 (2020).
- [49] D. Dey and B. K. Patra, Phys. Rev. D **104**, 076021 (2021).
- [50] S. A. Khan and B. K. Patra, Phys. Rev. D **107**, no.7, 074034 (2023).
- [51] A. Das, H. Mishra and R. K. Mohapatra, Phys. Rev. D **102**, no.1, 014030 (2020).
- [52] J. R. Bhatt, A. Das and H. Mishra, Phys. Rev. D **99**, no.1, 014015 (2019).
- [53] S. Y. F. Liu and Y. Yin, Phys. Rev. D **104**, no.5, 054043 (2021).
- [54] B. Fu, L. Pang, H. Song and Y. Yin, [arXiv:2201.12970 [hep-ph]].
- [55] J. Cleymans and K. Redlich, Phys. Rev. C **60**, 054908 (1999).
- [56] F. Becattini, J. Cleymans, A. Keranen, E. Suhonen and K. Redlich, Phys. Rev. C **64**, 024901 (2001).
- [57] D. H. Rischke, M. I. Gorenstein, H. Stoecker and W. Greiner, Z. Phys. C **51**, 485-490 (1991).
- [58] A. Andronic, P. Braun-Munzinger, J. Stachel and M. Winn, Phys. Lett. B **718**, 80-85 (2012).
- [59] G. P. Kadam and H. Mishra, Phys. Rev. C **92**, no.3, 035203 (2015).
- [60] V. Vovchenko, M. I. Gorenstein and H. Stoecker, Phys. Rev. Lett. **118**, no.18, 182301 (2017).
- [61] V. Vovchenko, A. Motornenko, P. Alba, M. I. Gorenstein, L. M. Satarov and H. Stoecker, Phys. Rev. C **96**, no.4, 045202 (2017).
- [62] P. Huovinen and P. Petreczky, Phys. Lett. B **777**, 125-130 (2018).
- [63] S. Pal, G. Kadam and A. Bhattacharyya, [arXiv:2305.13212 [hep-ph]].
- [64] G. Kadam and H. Mishra, Phys. Rev. D **100**, no.7, 074015 (2019).
- [65] S. Pal, G. Kadam, H. Mishra and A. Bhattacharyya, Phys. Rev. D **103**, no.5, 054015 (2021).
- [66] K. A. Olive, Nucl. Phys. B **190**, 483-503 (1981).
- [67] J. Weil *et al.* [SMASH], Phys. Rev. C **94**, no.5, 054905 (2016).
- [68] S. R. De Groot, *Relativistic Kinetic Theory - Principles and Applications* (North-Holland Publishing Company, 1980).
- [69] P. Chakraborty and J. I. Kapusta, Phys. Rev. C **83**, 014906 (2011).
- [70] M. Albright and J. I. Kapusta, Phys. Rev. C **93**, no.1,

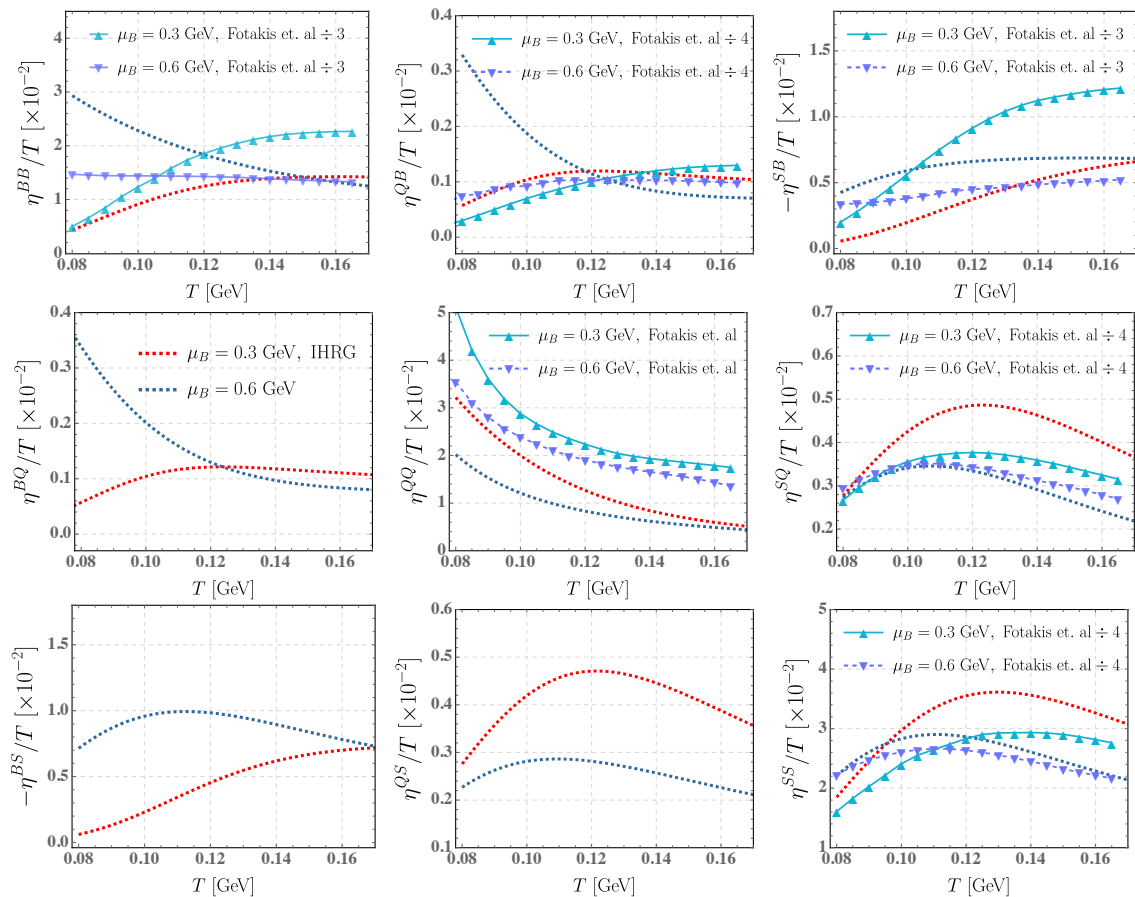


FIG. 12: The temperature dependence of the scaled thermoelectric transport coefficient matrix η^{qq}/T in baryon (top row), electric (middle row), strangeness diffusion current sectors (bottom row) at $\mu_B = 0.3$ GeV (red), 0.6 GeV (blue) using the IHRG model (dashed lines). These results are compared with the diffusion coefficient matrix result obtained by Fotakis *et al.* at $\mu_B = 0.3$ GeV (upper triangles) and 0.6 GeV (lower triangles) with the same settings ($n_S = 0, \mu_Q = 0$) [41].

- 014903 (2016).
- [71] J. L. Anderson and H. R. Witting, *Physica* **74**, 466 (1974).
- [72] J. A. Fotakis, E. Molnár, H. Niemi, C. Greiner and D. H. Rischke, *Phys. Rev. D* **106**, no.3, 036009 (2022).
- [73] E. Molnar, H. Niemi and D. H. Rischke, *Phys. Rev. D* **93**, no.11, 114025 (2016).
- [74] R. Derradi de Souza, T. Koide and T. Kodama, *Prog. Part. Nucl. Phys.* **86**, 35-85 (2016).
- [75] Callen, H. B. *The Application of Onsager's Reciprocal Relations to Thermoelectric, Thermomagnetic, and Galvanomagnetic Effects*. *Physical Review*, 73(11), 1349-1358 (1948).
- [76] Redin, R. D., *Thermomagnetic and galvanomagnetic effects* (1957). Ames Laboratory ISC Technical Reports. 176.
- [77] A. B. Larionov, O. Buss, K. Gallmeister and U. Mosel, *Phys. Rev. C* **76**, 044909 (2007).
- [78] M. E. Peskin and D. V. Schroeder, *An Introduction to quantum field theory*, Addison-Wesley, 1995, ISBN 978-0-201-50397-5.
- [79] C. Greiner, P. Koch and H. Stoecker, *Phys. Rev. Lett.* **58**, 1825-1828 (1987).
- [80] J. Cleymans and H. Satz, *Z. Phys. C* **57**, 135-148 (1993).
- [81] V. Vovchenko and H. Stoecker, *Comput. Phys. Commun.* **244**, 295-310 (2019).
- [82] J. Cleymans, H. Oeschler, K. Redlich and S. Wheaton, *Phys. Rev. C* **73**, 034905 (2006).
- [83] G. Odyniec, *J. Phys. Conf. Ser.* **455**, 012037 (2013).
- [84] B. Aboona *et al.* [STAR], *Phys. Rev. Lett.* **130**, no.8, 082301 (2023).
- [85] J. Hammelmann, J. Staudenmaier and H. Elfner, [[arXiv:2307.15606](https://arxiv.org/abs/2307.15606) [nucl-th]].
- [86] J. Grefa, M. Hippert, J. Noronha, J. Noronha-Hostler, I. Portillo, C. Ratti and R. Rougemont, *Phys. Rev. D* **106**, no.3, 034024 (2022).
- [87] R. Rougemont, J. Noronha and J. Noronha-Hostler, *Phys. Rev. Lett.* **115**, no.20, 202301 (2015).
- [88] W. T. Deng and X. G. Huang, *Phys. Rev. C* **85**, 044907 (2012).
- [89] A. Das, H. Mishra and R. K. Mohapatra, *Phys. Rev. D* **99**, no.9, 094031 (2019).
- [90] A. Das, H. Mishra and R. K. Mohapatra, *Phys. Rev. D* **101**, no.3, 034027 (2020).